Turkish Journal of Earth Sciences (Turkish J. Earth Sci.), Vol. 21, 2012, pp. 497–520. Copyright ©TÜBİTAK
doi:10.3906/yer-0910-27 First published online 23 August 2010

Kinematics and Basin Formation Along the Ezinepazar-Sungurlu Fault Zone, NE Anatolia, Turkey

M. KORHAN ERTURAÇ[1,2] & OKAN TÜYSÜZ[1]

[1] Eurasian Institute of Earth Sciences, İstanbul Technical University, Maslak, TR–34469 İstanbul, Turkey
[2] Present Address: Sakarya University, Department of Geography, Esentepe Campus, Serdivan, TR–54187 Sakarya, Turkey (E-mail: erturac@sakarya.edu.tr)

Received 16 October 2009; revised typescripts receipt 19 April 2010 & 03 August 2010; accepted 23 August 2010

Abstract: The Ezinepazar-Sungurlu Fault (EzSF) is a major offshoot of the dextral North Anatolian Fault (NAF) zone, which bifurcates from the main fault strand around the Niksar pull-apart basin (37°E) and strikes through the Central Anatolian Block for 200 km to the west (34°E). The easternmost segment of the EzSF, the Ezinepazar Fault (EzF), which ruptured during the 1939 Erzincan earthquake (Mw= 7.8), has a very remarkable expression as a single-strand fault. Micromammal dating of young sediments along this segment indicate that the EzF was initiated during the Middle Pleistocene (0.7–1 Ma) and propagated westward accumulating 6.5±0.5 km maximum morphological offset. The central segment of the EzSF, the Deliçay Fault (DF), is expressed as an en-échelon pattern and controlled the formation of a narrow fault-wedge basin (Aydınca Plain). The stepover between the DF and its western continuation, the Geldingen Fault (GF), forms a young pull-apart basin (Geldingen Basin) where the maximum morphological offset is measured at 3.5±1 km. In the westernmost part of the fault zone, the deformation zone widens and the EzSF bifurcates into the Mecitözü (MF) and the Sungurlu faults (SF). The MF controlled the deposition of continental clastics, dated as Late Miocene–Early Pliocene by using mammal chronology (MN13-14). The Neogene–Quaternary stratigraphy of the basins along the EzSF indicates two phases of faulting-related basin formation. The first period took part during the Late Miocene–Early Pliocene; the second phase started with the initiation of the EzF in the east during the Middle Pleistocene. The western propagation of the fault caused the reactivation of older tectonic lines as an element of the NAF system. The offset distribution measured along the EzSF shows that accumulated long-term slip is not uniform along the fault, as it decreases gradually where the fault becomes distant from the NAF main strand. This projection is applicable to present day slip rate distribution along the EzSF, which is shown also by GPS measurements and is therefore important for earthquake hazard estimates for the region.

Key Words: North Anatolian Fault, Ezinepazar-Sungurlu Fault, morphotectonics, splay faulting, Amasya Basin

Ezinepazar-Sungurlu Fayının Evrimi, Kinematiği ve Havza Oluşumu, KD Anadolu, Türkiye

Özet: Ezinepazar-Sungurlu Fayı (EzSF), Kuzey Anadolu Fay (KAF) hattından ayrılan önemli bir yan koludur. Bu fay, Niksar yakınlarında (37°D) anakoldan ayrılarak Anadolu Blok'unun içlerine doğru, yaklaşık 200 km boyunca (34°D), belirgin olarak izlenir. EzSF'nin en doğu kesimi olan Ezinepazar Fayı (EzF) çarpıcı bir aktif fay morfolojisine sahiptir ve bu kol 1939 Erzincan (Mw= 7.8) depreminde tamamen kırılmıştır. Bu segmentin üzerinde gelişmiş havzalarda depolanan genç çökellerin mikromemeli yaşlandırması, fayın oluşumunun Orta Pleyistosen'de (0.7–1 My) başladığını göstermektedir ve bu dönem içerisinde doğuda en çok 6.5±0.5 km morfolojik ötelenme birikmiştir. EzSF'nin orta segmentini oluşturan Deliçay Fayı (DF), belirgin bir '*en-échelon*' geometrisi sunarak dar bir dağ önü ovasının gelişimini kontrol etmiştir. DF ve batı devamı olan Geldingen Fayı (GF) arasında gerçekleşen sağ yönlü sıçrama ve ölçülen 3.5±1 km morfolojik atım, genç bir çek-ayır havzanın oluşumunu denetler. EzSF en batı kesiminde, Mecitözü Fayı (MF) ve Sungurlu Fayı (SF) olarak iki kola ayrılmaktadır. Bu faylar, mikromemeli fosilleri ile Geç Miyosen–Erken Pliyosen aralığında yaşlandırılan karasal bir çökel paketinin depolanmasını kontrol etmişlerdir.

EzSF üzerinde bulunan havzaların Neojen–Kuvaterner stratigrafisi iki farklı evrede fay kontrollü havza oluşumunu işaret etmektedir. İlk dönem, Geç Miyosen–Erken Pliyosen döneminde aktif olmuştur. İkinci dönem, Ezinepazar Fayı'nın Orta Pleyistosen'deki oluşumuyla başlayarak, doğudan batıya doğru ilerlemesi sonucu görece eski tektonik hatları sağ yanal KAF sistemi içerisinde yeniden harekete geçirmesi ile tanımlanmışır. Fay üzerinde ölçülen morfolojik ötelenmelerin fay boyunca azalarak sistemin en batı kesiminde tamamen sonlanması, fayın üstündeki kayma hızının oluşumdan günümüze sabit olmadığını göstermektedir. Bu yorum GPS verileri ile desteklenmekte ve bölgenin deprem tehlike analizi çalışmaları için önem arzetmektedir.

Anahtar Sözcükler: Kuzey Anadolu Fayı, Ezinepazar-Sungurlu Fayı, morfotektonik, Amasya Havzası

Introduction

The North Anatolian Fault (NAF; Ketin 1957; Allen 1969; Ambraseys 1970; Şengör 1979; Barka 1992; Herece & Akay 2003) is one of the most active continental strike-slip faults in the world. It has a very remarkable morphological expression along its ~1400-km-long course and has almost completely ruptured with nine westward propagating destructive earthquakes starting in 1939 with Erzincan (Mw= 7.8) event and followed by the 1942 Niksar-Erbaa (M= 7.2); 1943 Tosya (Mw= 7.4); 1944 Gerede (M= 7.5), 1951 Kurşunlu (M= 6.8), 1957 Abant (M= 6.8), 1967 Mudurnu (M= 7.0) (Barka 1996) and most recently the 1999 İzmit (Mw= 7.4) (Barka *et al.* 2002) and Düzce (Mw= 7.2) (Akyüz *et al.* 2002) events. The NAF has a dextral sense of slip and is accepted as forming the northern boundary of the Anatolian Block during the Late Miocene, after continental collision of the Arabian and Eurasian plates (Şengör 1979; Armijo *et al.* 1999; Okay *et al.* 2010) causing westward migration (McKenzie 1972) and counterclockwise rotation (Rotstein 1984) of the Anatolian Plate. Modelling of GPS data defines this rotation as nearly rigid, around a pole in the Sinai Peninsula with a 24±1 mm/yr uniform slip-rate along the NAF (McClusky *et al.* 2000; Reilinger *et al.* 2006). This is also shown by long-term geological slip rate studies, where the NAF is expressed as a single fault strand (20.5±5.5 mm/yr for the Eksik segment; Kozacı *et al.* 2007; E in Figure 1).

However, microseismic activity and related active deformation within the Anatolian Block are mainly concentrated along some linear features, which are generally connected to NAF as splays (Figures 1 & 2). In a recent review on the NAF, Şengör *et al.* (2005) described a broad active deformation zone along the northern Anatolian block (North Anatolian Shear Zone, NASZ), with the NAF as the most prominent element. The NASZ is developed following the older structures within an accretionary complex, which was created by closure of the Tethys Ocean and its branches (Şengör *et al.* 2005). There is a strong correlation between the width of the NASZ and the branching-off from the NAF as it follows a straight course in an area where the NASZ is narrow, except for small-scale stepovers and superimposed basins formed during the evolution of the fault zone (e.g., Barka 1985; Koçyiğit 1989, 1990, 1996; Gürer *et al.* 2006). However, systematic offshoots can be seen in areas where the accretionary complex widens. These wide zones of secondary fault zones (splays), with many synthetic and antithetic branches are very distinct in two regions along the NASZ (Kim & Sanderson 2004; Şengör *et al.* 2005) (i) the Sea of Marmara region in the west and (ii) the Amasya region in the central convex part of the NAF (SoM and ASZ in Figure 1 respectively). Recent studies by Meade *et al.* (2002) and Flerit *et al.* (2003), based on the densely distributed GPS network around the SoM region, where the NAF shows a branched network of active faults, claim that although the northern branch is more distinctive and is known to have created destructive historical earthquakes, at least 20% of the plate motion around the SoM occurs along the southern branch. Besides, the studies along the Düzce Fault, a major splay ruptured during the 1999 Düzce earthquake (Akyüz *et al.* 2002), defined the long-term geological slip rate of the Düzce Fault as 15.0±3.2 mm/yr (Pucci *et al.* 2008; D in Figure 1). There are also individual splay zones, regarded as recent and former contributors to the long-term deformation of the Anatolian Plate (e.g., Almus Fault, Bozkurt & Koçyiğit 1995, 1996; Tosya Fault, Dhont *et al.* 1998; Central Anatolian Fault, Koçyiğit & Beyhan 1998; Ovacık Fault, Barka & Gülen 1989; Westaway & Arger 2001; Figure 1), which have created unexpected destructive earthquakes during both the historical and instrumental periods (e.g., Mw: 6.0 Orta earthquake, Koçyiğit *et al.* 2001; Çakır & Akoğlu 2008) and were reported in previous studies (see the Active Tectonic Map of Turkey by Şaroğlu *et al.* 1992 and Bozkurt 2001 for a review). These studies advocate that present day slip-rates along the NAF are partitioned between major and minor fault segments and therefore contradict uniform slip models discounting internal deformation of the Anatolian plate.

In a narrow nucleation zone located around Niksar Town (37°E), two major secondary fault zones (splays) bifurcate successively from the main fault strand. These faults show a single-sided fishbone-like structure within the central convex bend of the NAF and strike through the Central Anatolian Block for at least 200 km to the west (Figure 2). Both the southern splay, (Ezinepazar-Sungurlu Fault, EzSF),

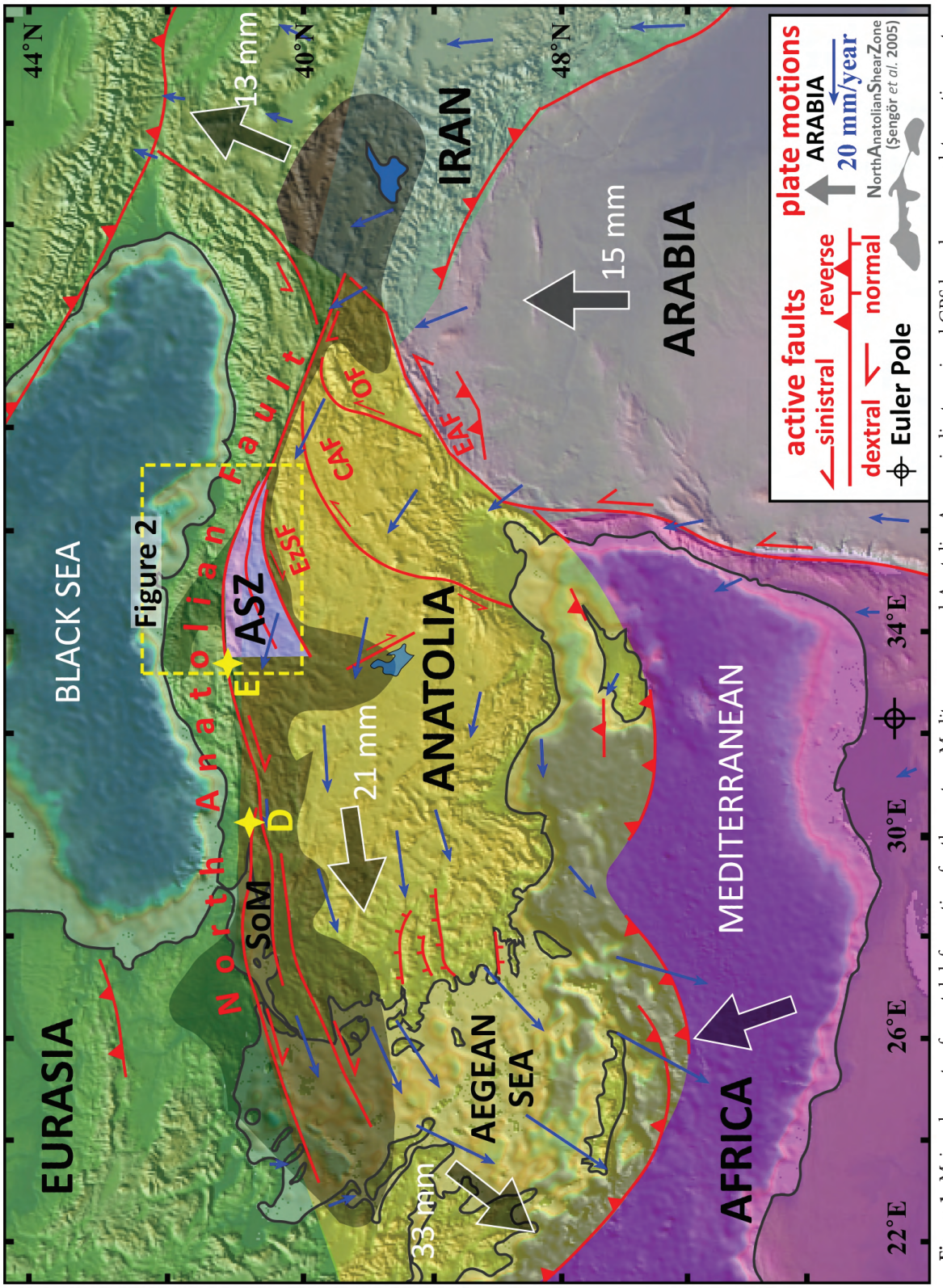

Figure 1. Major elements of crustal deformation for the eastern Mediterranean and Anatolia. Arrows indicate regional GPS based average plate motion vectors (Reilinger *et al.* 2006). Grey shaded area corresponds to the distribution of the North Anatolian Tethyside accretionary complexes (North Anatolian Shear Zone of Şengör *et al.* 2005). SoM– Sea of Marmara, ASZ– Amasya Shear Zone, EzSF– Ezinepazar-Sungurlu Fault, CAF– Central Anatolian Fault, OF– Ovacık Fault, EAF– East Anatolian Fault.

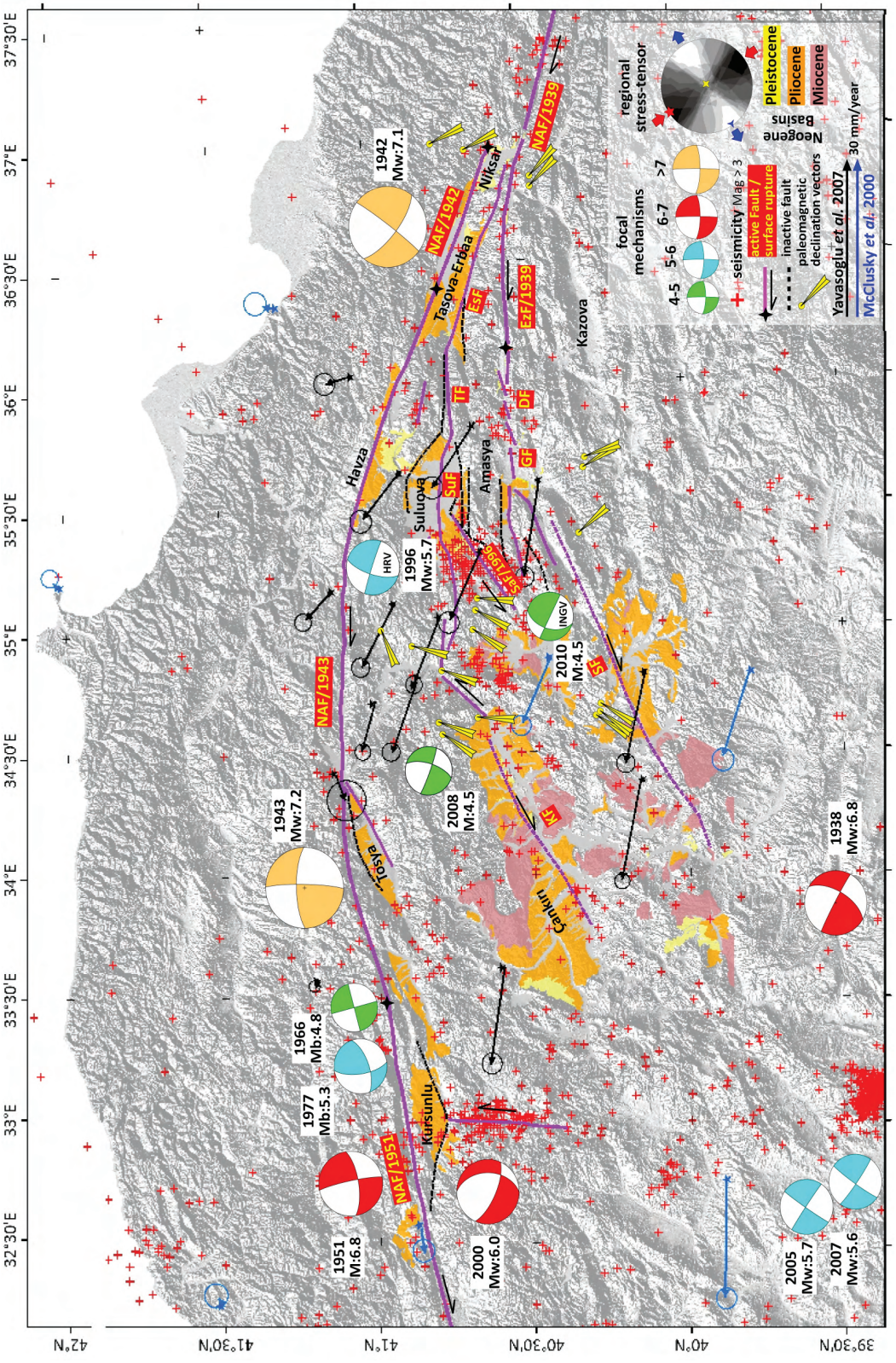

Figure 2 . Detailed look at the ASZ with active faults, Neogene sedimentary basins (compiled from Tüysüz *et al.* 1998; Kaymakcı 2000; Herece & Akay 2003; Erturaç 2009), micro and macro seismicity (ISC & KOERI Catalogues), GPS velocity vectors (McClusky *et al.* 2000; Yavaşoğlu *et al.* 2007), mean palaeomagnetic declination vectors of Eocene volcanics (Tatar *et al.* 1995; İşseven & Tüysüz 2006). Regional stress tensor (σ_1= 126°/03°, σ_2= 269°/86°, σ_3= 035°/03°) is from Kiratzi (2002) and presented with a right dihedra diagram (Ramsey & Lisle 2000), using the catalogue of the focal mechanism solutions of well known earthquakes (Tan *et al.* 2008) and for more recent events (from Çakır & Akoğlu 2008; Erturaç *et al.* 2009; Tan *et al.* 2010; INGV 2010). Abbreviations; NAF– North Anatolian Fault, EzF– Ezinepazar Fault, DF– Deliçay Fault, GF– Geldingen Fault, SF– Sungurlu Fault, EsF– Esençay Fault, TF– Taşova Fault, SuF– Suluova Fault, SaF– Salhan Fault, KF– Kızılırmak Fault.

and the central splay (Esençay-Taşova-Suluova-Kızılırmak faults) with many related synthetic and antithetic branches, deforms a broad wedge-shaped area, the Amasya Shear Zone (ASZ), delimited by the main trunk of the NAF and the EzSF (Figure 2). This system of active deformation hosts remarkable morphotectonic features, such as elongated basins (e.g., the Taşova-Erbaa, Havza, Suluova and Amasya basins) and narrow uplifts (e.g., the Akdağ, Tavşan, Sakarat and Karadağ mountains) accompanied by distributed microseismic activity and has produced moderate earthquakes during the instrumental period, such as the 1942 Kızılırmak Valley events (Mw= 5.6–6.0; Eyidoğan *et al.* 1991); 1996 Salhan (Mw= 5.6; Pınar *et al.* 1998) and 2005–2008 Çorum (M= 4.2–4.5; KOERI) events (Figure 2).

The ASZ has developed on the easternmost portion of the Sakarya Continent, the Tokat Massif (TM; Blumenthal 1950; Şengör & Yılmaz 1981; Rojay 1993, 1995; Tüysüz 1996; Yılmaz *et al.* 1997; Yılmaz & Yılmaz 2004), which is bounded by the Çankırı Basin to the west, the Ankara-Erzincan suture to the south and the NAF master strand to the north. The pre-Neogene rocks of the TM consist of 4 different groups, which are separated from each other by regional unconformities (Tüysüz *et al.* 1998). These are: (1) the metamorphic basement – the Triassic Karakaya complex, (2) Liassic to Lower Cretaceous clastics, volcanics and carbonate rocks, (3) Upper Cretaceous blocky limestones, ophiolites and volcanics, (4) Eocene sedimentary and volcanic rocks. The complicated geological evolution of the TM from the Triassic to Neogene epochs (Yılmaz *et al.* 1997; Yılmaz & Yılmaz 2004) led to the formation of mostly E–W-oriented faults and north-vergent thrusts, forming a distributed discontinuity network aligned almost parallel to the active faults of the ASZ (Figure 3). Moreover, Yılmaz & Yılmaz (2004) claimed that these thrust faults were reactivated during the Neotectonic regime.

The palaeomagnetic declinations derived from the Eocene volcanic rocks indicates two distinct regions of rotation close to the ASZ (Tatar *et al.* 1995; İşseven & Tüysüz 2006; Figure 2): (i) Counterclockwise rotations located south of the EzSF compatible with the GPS-derived rotation of the Anatolian block and (ii) clockwise rotations within the ASZ consistent with the expected rotation of a continental block bounded by two dextral faults (McKenzie & Jackson 1986; İşseven & Tüysüz 2006).

The southern border of the ASZ, the ~200-km-long EzSF (Figure 3), is the main focus of this study. Recognition of EzSF extends back to the field surveys after the 1939 Erzincan (Ms= 7.9) earthquake (Parejas *et al.* 1941; Ketin 1969). Later, the fault zone was mentioned in key papers on the NAFZ (Şengör 1979; Şengör *et al.* 1985, 2005; Barka & Kadinsky-Cade 1988; Koçyiğit 1990; Barka 1992, 1996; Suzanne & Lyberis 1992; Tatar *et al.* 1995; Bozkurt 2001) and mapped at a particular scale (1/100.000) within the extent of the geological maps of various interests (Karaalioğlu 1978, 1983; Aktimur *et al.* 1992; Tüysüz 1992) and the Active Fault Map of Turkey (Şaroğlu *et al.* 1992). Different parts of the EzSF were studied by different researchers (Polat 1988; Kaymakcı 2000; Koçbulut 2003). Recently, the EzSF was interpreted as a key structure in understanding the tectonic evolution of the eastern NAFZ (Şengör & Barka 1992; Barka *et al.* 2000; Özden *et al.* 2002) and the internal deformation of the northeastern Anatolian Block (Kaymakcı 2000; Seyitoğlu *et al.* 2000, 2009; Kaymakcı *et al.* 2003, 2010; Koçbulut 2003; Koçyiğit 2003) All the cited literature above regards the EzSF as a dextral fault zone.

In this study, a detailed mapping survey, aided with 1/15.000 scale aerial photos and digital elevation models, was undertaken to understand the characteristics of the EzSF. To establish the architecture of the Neogene–Quaternary basins developed along the fault zone, temporal and spatial relationships between different sedimentary units were constructed by using mammal palaeontology and OSL (optically stimulated luminescence) dating. Microfault measurements within these sediments were used in kinematic analysis to understand the stress tensor and spatial change in the principal stress axis along the fault zone.

Ezinepazar-Sungurlu Fault (EzSF)

The EzSF is divided into five fault segments based on major changes in the fault geometry and kinematics (Figure 3). The easternmost segment, the 60-km-long Ezinepazar segment, which ruptured during the 1939

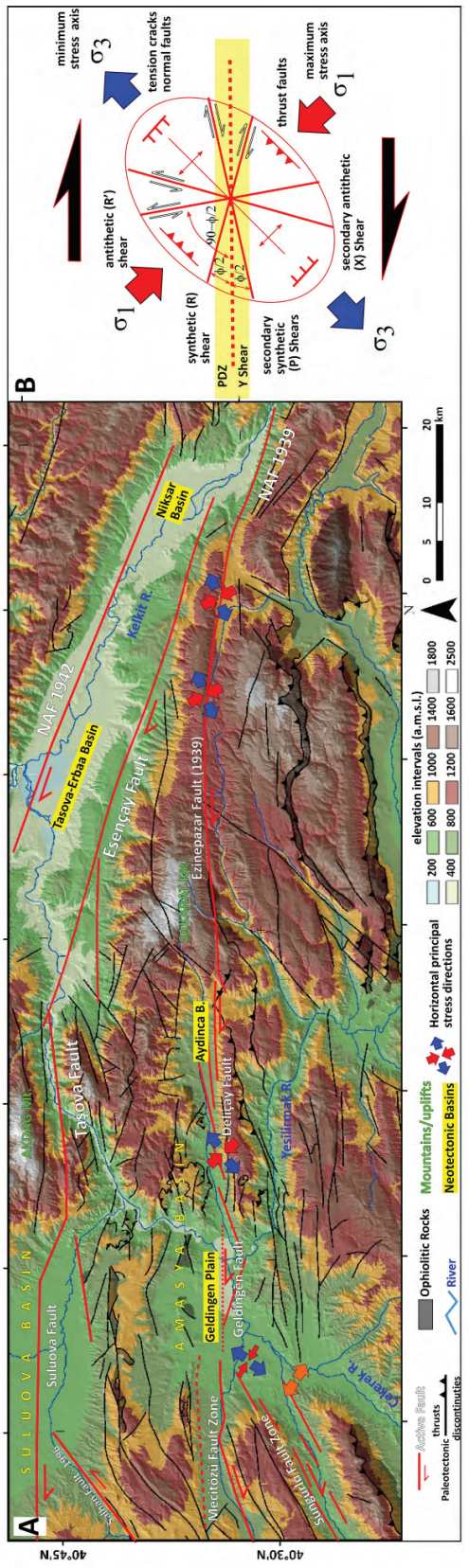

Figure 3. (A) Morphotectonic elements (basins and uplifts), active fault segmentation and stress tensor evaluations along the EzSFZ. Note that the general trend of inactive faults of the Palaeotectonic regime and the distribution of ophiolitic rocks (compiled from Yilmaz *et al.* 1997; Tüysüz *et al.* 1998; Şenel 2002) show great alignment with recent faulting (red lines), indicating that active faults are indeed replacement structures following older damage zones. **(B)** Riedel fracture geometry of a E-trending dextral shear zone formed under the control of NW-directed maximum and NE-directed minimum horizontal shear stresses (redrawn after Tchalenko 1970; Dresen 1991).

Erzincan earthquake (Mw= 7.8), forms a smooth bend as it changes its strike from N105°E to E–W at its centre (Figure 3). The western continuation of this segment to the south of Amasya city shows an en-échelon pattern (Deliçay segment) forming a narrow basin (Aydınca Plain), and then is followed by a right-handed stepover (Geldingen segment) forming the Geldingen pull-apart basin. These sedimentary basins are connected to each other by the Yeşilırmak drainage network and together form the Amasya Basin (Figure 3). The westernmost continuation of the EzSF is rather complicated as it branches again at the end of the Geldingen Plain into the E–W-trending Mecitözü and N65°E trending Sungurlu segments (Figure 3). Only three eastern segments will be described in detail in this paper.

Ezinepazar Segment (EzF)

The easternmost part of the EzSF, the Ezinepazar segment (EzF), starts as the western continuation of the NAF near Umurlu Village (Figure 4), where the main strand makes a large right-handed dilatational stepover, forming the Niksar sigmoidal pull-apart basin (Mann *et al.* 1983; Hempton & Dunne 1984; Aktimur *et al.* 1992; Tatar 1996). This segment has a very distinct and fresh morphological expression among the highlands with an average altitude of ~1100 m. The EzF was entirely ruptured during the 1939 Erzincan earthquake (Parejas *et al.* 1941; Ketin 1957; Ambraseys 1970). The fault rupture of this segment was 65 km long and the measured dextral co-seismic slip was about 1.5–2 metres (Barka 1996). The segment ends at Girap Village (Figures 4 & 6), where the 1939 rupture terminates with a compressional imbricating fan, which acted as an earthquake barrier (Barka & Kadinsky-Cade 1988). The nucleation zone of the EzF, the Niksar Basin, is actually composed of three adjacent pull-apart basins formed due to its geometry and interactions between active segments of the NAF. Those are from south to north (i) slight (1 km in width) bending between the Kelkit segment of the NAF and the Ezinepazar segment, forming the Umurlu Plain (ii) an ~3.5 km stepover between the EzF and Esençay Fault (EsF), forming the Boğazbaşı Plain, and (iii) an ~8.5 km stepover between the EsF and the main strand of the NAF (surface rupture of the 1942 Earthquake) forming the Niksar Basin. The age of the Umurlu Plain is ~0.6–0.7 Ma (Toringian), constrained by the discovery of a *Microtus* aff. *arvalis* rodent (for timing constraints see Sala & Masini 2006) within intensely sheared and deflected river clastics near Umurlu Village. This age correlates well with the dates of the Niksar volcanics (568±3–461±7 Ka, K-Ar), which erupted using the NAF as a conduit (Tatar *et al.* 2007). These ages also indicate the timing of initiation of the EzF, which is thought to be synchronous with the opening of the Niksar pull-apart basin (Barka *et al.* 2000; Adıyaman *et al.* 2001; Tatar *et al.* 2007), constrained within the last 1–0.7 Ma.

The EzF cuts through the Mt. Sakarat uplift, which is the footwall of the Taşova-Erbaa Basin, where NE-facing slopes drain to the Kelkit River and SW-facing slopes drain to the Yeşilırmak River (Figure 4). Today, this uplift and related drainage network are seen to be dissected and diverted especially in the eastern part by recent fault activity, where the EzF is dipping north and has a reverse component, as indicated by wind gaps north of the Avlunlar Plain. In the west, the river network shows a highly disturbed geometry, mostly running through shear-controlled east-trending valleys. Geometry and long-term slip along the fault led to the development of river offsets, captures and also disconnections, where at least two of the outlets are separated from active flow due to linear rises created by the south-dipping reverse component of the fault (Figure 4). In the central part of the segment (Gölönü Village) the Kelkit catchment appears to be advancing southwards, causing recent captures from the Yeşilırmak catchment. This is probably due to the interaction between the Ezinepazar and Esençay faults, causing the Mt. Sakarat block to tilt northward (Figure 4).

Figure 5 is a close-up view of the central portion of the EzF (Gölönü-Fındıcak villages) showing the active morphological signature of the fault zone with recent river and alluvial fan deflections, river captures, triangular facets, pressure ridges and sag-ponds. There are also complicated pressure ridges (such as the sigmoidal Fındıcak hill; see McClay & Bonora 2001) where the geometry of these features indicates that EzF acts under NE–SW extensional and NW–SE compressional stresses, which is also shown by faulting data observed in this study (Umurlu) and

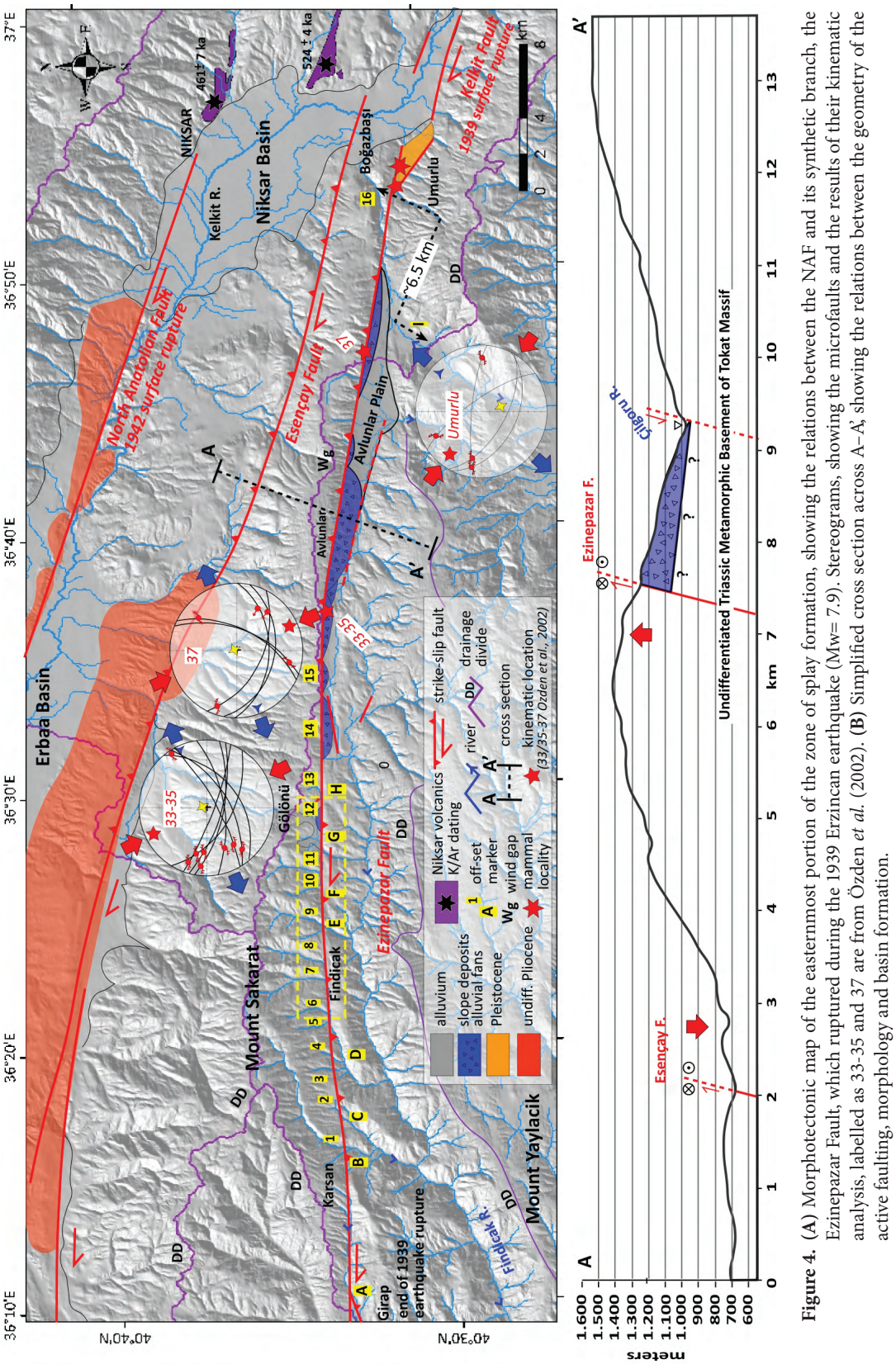

Figure 4. (**A**) Morphotectonic map of the easternmost portion of the zone of splay formation, showing the relations between the NAF and its synthetic branch, the Ezinepazar Fault, which ruptured during the 1939 Erzincan earthquake (Mw= 7.9). Stereograms, showing the microfaults and the results of their kinematic analysis, labelled as 33-35 and 37 are from Özden *et al.* (2002). (**B**) Simplified cross section across A–A', showing the relations between the geometry of the active faulting, morphology and basin formation.

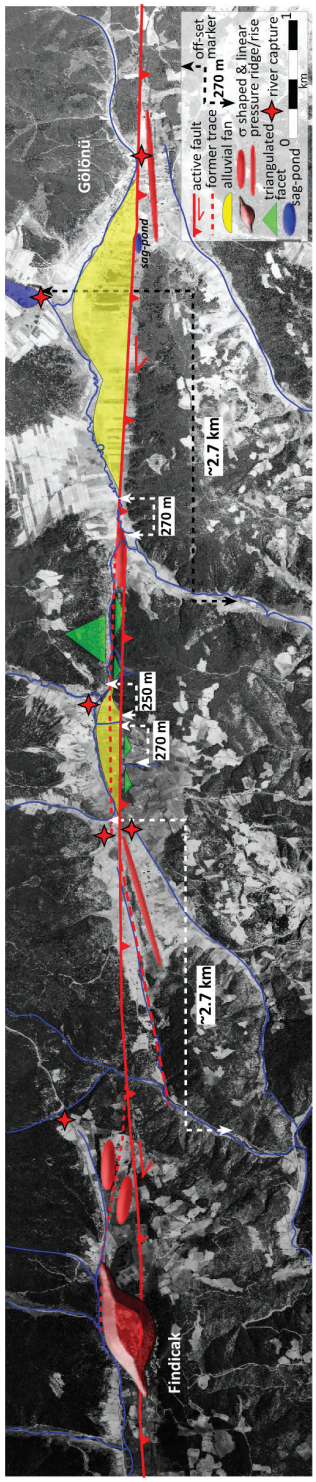

Figure 5. Interpretation of a 1/15.000-scaled aerial photo, covering an area between Fındıcak and Gölönü villages, showing examples of distinct morphological elements formed by the continuous evolution and temporal geometrical changes of the fault trace by means of dextral slip.

previously published kinematic datasets (Tatar 1996; Özden *et al.* 2002).

Only a few small depositional areas formed along the EzF, such as the wedge-shaped Avlunlar Plain, due to the straight and continuous fault pattern of the EzF, except some small stepovers forming sag-ponds and compressional ridges. Sedimentary fill of the Avlunlar Plain is mostly composed of coarse clastics derived from the active northern border, accompanied by alluvial fans and fluvial deposits of the Çılgöru River in the east (Figure 4B). The contact between the basement rocks and sedimentary fill is exposed in sections in the Çılgörü River, allowing us to calculate the maximum sediment thickness as 100 m.

As similar low-grade metamorphic rocks of the TM (Yılmaz *et al.* 1997; Yılmaz & Yılmaz 2004) form the northern and southern blocks of the EzF, it was not possible to use geological contacts as offset markers, although morphological markers seem to be enough for cumulative slip estimations. For this purpose, all the outlets and their tributaries (located on the southern and northern blocks) forming the complex river network of the region have been matched together along the fault using the methodology described in Huang (1993). Among the 38 measurements, ranging from ~2 to 8 km (Figure 4), the most constrained dextral offset created by the EzF is located at the easternmost part as 6.5±0.5 km (Figure 4 / I-6). This offset probably accumulated during a maximum of ~1–0.7 Ma, as constrained by the age of the Niksar Basin: therefore we can estimate an ~7–10 mm/year long-term slip rate for the EzF, the easternmost portion of EzSF.

Deliçay Segment (DF)

In contrast to the EzF, the western continuation (central part) of the EzSF, the Deliçay segment (DF), shows an en-échelon pattern and significant changes in its geometry along its ~30 km course. This change is marked by the Kaleköy Gorge, in the centre of the segment. In the eastern part, the strike of the fault gradually changes from E–W to N70°E by making small right-handed stepovers (Figure 6). This geometry is in the typical helicoidal form of Riedel fractures (Naylor *et al.* 1986), and controls

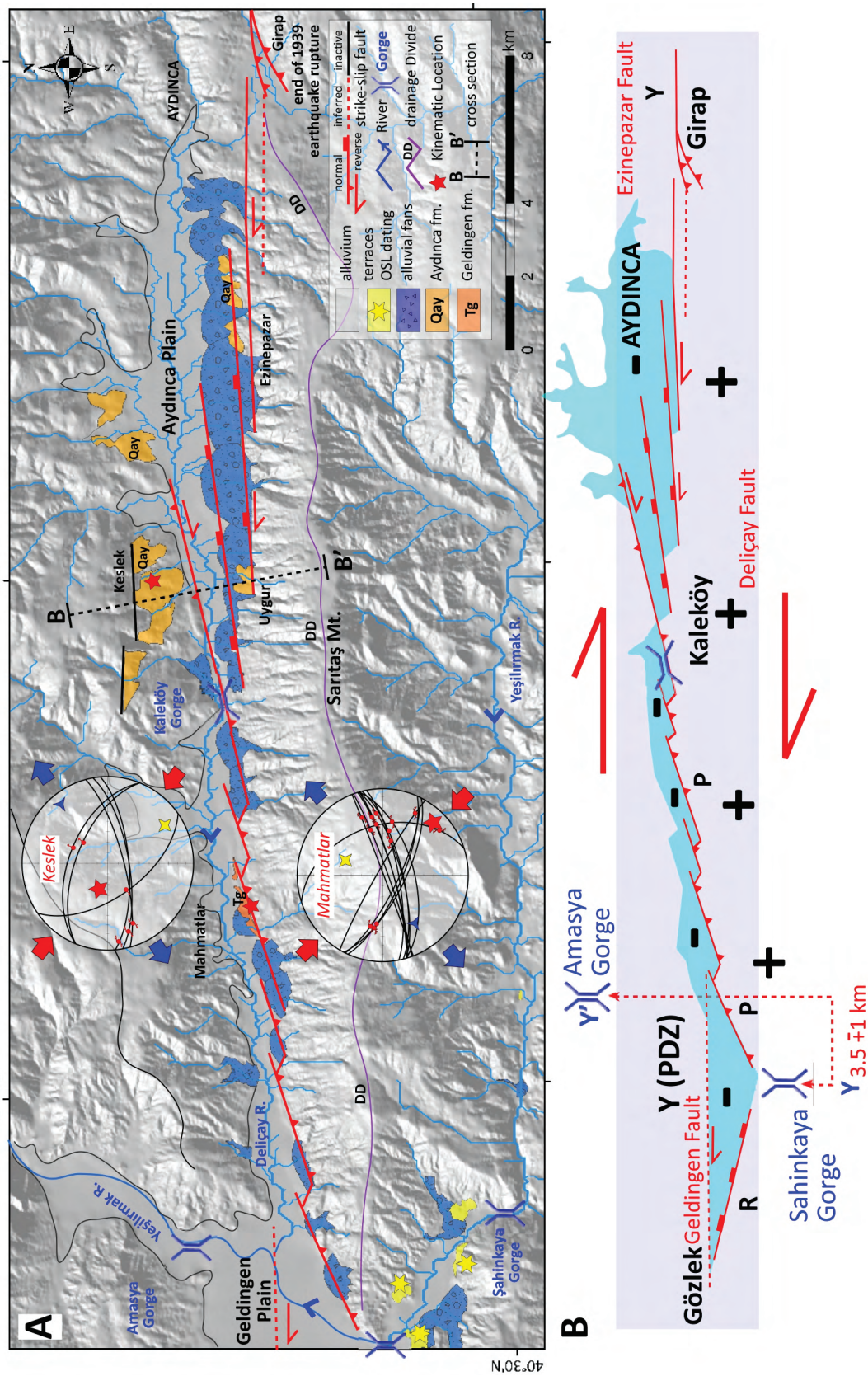

Figure 6. (A) Morphotectonic map of the Deliçay Segment of the EzSF. The changes in the geometry along the strike of the fault caused the formation of a narrow fault-wedge piedmont basin (Aydınca Plain) where continuous sedimentation took place from the Middle–Late Pleistocene to the Recent. The saw-tooth-like segmented fault geometry west of the Kaleköy Gorge caused compression and uplift of the southern block. Stereograms show the measured microfaults (Keşlek and Mahmatlar stations) and the results of the kinematic analysis. **(B)** Simplified fault geometry and related basin evolution model along the DF and GF; notations attributed to the each segment indicate Riedel fault geometry terminology (Dresen 1991). Note the 3.5±1 km dextral offset of the Yeşilırmak River achieved by cutting two gorges located both south and north of the EzSF.

the geometry of the Aydınca Plain, which is a fault-wedge basin with a principal displacement zone in the south (Christie-Blick & Biddle 1985; Koçyiğit 1989). From the Kaleköy Gorge to the Geldingen Plain, the western part of the DF shows a saw-tooth trajectory, similar to the 1999 Düzce earthquake surface rupture (Pucci *et al.* 2006), formed by combination of P and R shears of the Riedel fracture geometry (Tchalenko 1970).

The kinematics of the DF were determined by analyzing striated fault surfaces measured in two stations within the Neogene sediments (Figure 6A). The Keşlek dataset, located in the north-central part of the fault zone, is composed of three ENE-trending, south-dipping oblique (dextral with normal component) faults and three NW-trending conjugate normal faults. The Mahmatlar dataset, however, is geometrically similar to the Keşlek station but this time dextral faults have a reverse component. Analysis of these two datasets implies that the DF evolved under NE-directed extensional and NW-directed compressional stresses indicating a pure E–W-trending principal deformation zone (Figures 5 & 11). The analysis also shows that the DF is transtensional in the east and transpressional in the west, which is compatible with the fault zone geometry.

The oldest Neogene unit cropping out along the DF is the Upper Miocene–Lower Pliocene Geldingen formation (Figure 6). Limited outcrops of this formation were observed west of the Kaleköy Gorge, around Mahmatlar Village and consist mainly of intensely sheared fluvial clastics. Recent alluvial fans unconformably overlie this unit. The sedimentary record of the Aydınca Basin indicates that there is a gap in the sedimentation before the second distinctive unit, the Aydınca formation (Qay), was deposited as an alluvial fan network distributed along the northern and southern sides of the DF. Formation of this unit is controlled by oblique faulting and rests unconformably on the basement rocks of the region (Figure 7).

This formation evolved in three phases accompanied by gradual subsidence of a piedmont basin. In the first phase, starting at ~700 m above mean sea level (amsl), an alluvial fan was deposited; recording lithofacies proximal to distal parts (Figure 7). These fan clastics, resting unconformably on the Triassic metamorphic units, start with immature, boulder-size clasts (Figure 7A–C). Up section, clasts become gradually smaller and rounded, then the beds are cut by channel deposits which grade up into cross- and parallel-laminated fine sands and gravels intercalated with red clays (Figure 7D, E). Palaeocurrent analysis of imbricated clasts indicates that the primary sediment source was in the north and clast lithology is mostly formed from intermediate to mafic volcanics (mostly andesites), which probably derived from the Upper Cretaceous volcanics of the Lokman formation (Alp 1972; Tüysüz 1992, 1996) cropping out north of the Aydınca Plain. This south-facing fan sedimentation was probably triggered by propagation of the EzSF east of Aydınca town. Limited outcrops of the southern equivalent of this phase, consisting of grey to brown massive clays (Figure 7G), can be observed south of Aydınca.

The second phase started to develop at ~640 metres (amsl), simultaneously or just after the erosion of the first phase. During this phase dominantly alluvial fans were deposited along the southern border of the Aydınca Plain (Figure 7H). They unconformably overlie both the basement rocks and the Geldingen formation. The clasts are mostly phyllite and marbles of the Triassic metamorphic rocks (Yeşilırmak metamorphites; Tüysüz 1996). Distal parts of these fans intercalate with fine clays and grade towards the centre of the basin into grey massive clays, currently being eroded by the Deliçay River (Figure 7F). The latest phase, which is still active, is identified using lithological descriptions of DSİ (Devlet Su İşleri, State Hydraulic Works) boreholes *53118* and *53962,* indicating an ~40 metre fluvial fill of the Deliçay River near the Kaleköy Gorge (Karaalioğlu 1978).

The sedimentary architecture of the Aydınca Plain was created by successive phases of sedimentation and erosion controlled by the progressive subsidence and extension of the basin. During depositional periods, alluvial fans developed close to the fault-controlled basin margins and shallow lake deposits accumulated in the basin centre. Change in colour of these sediments from red to grey is probably related to the primary clast source, indicating relative gradual subsidence in the basin that triggered rapid erosion at footwalls exposing the basement (Yeşilırmak

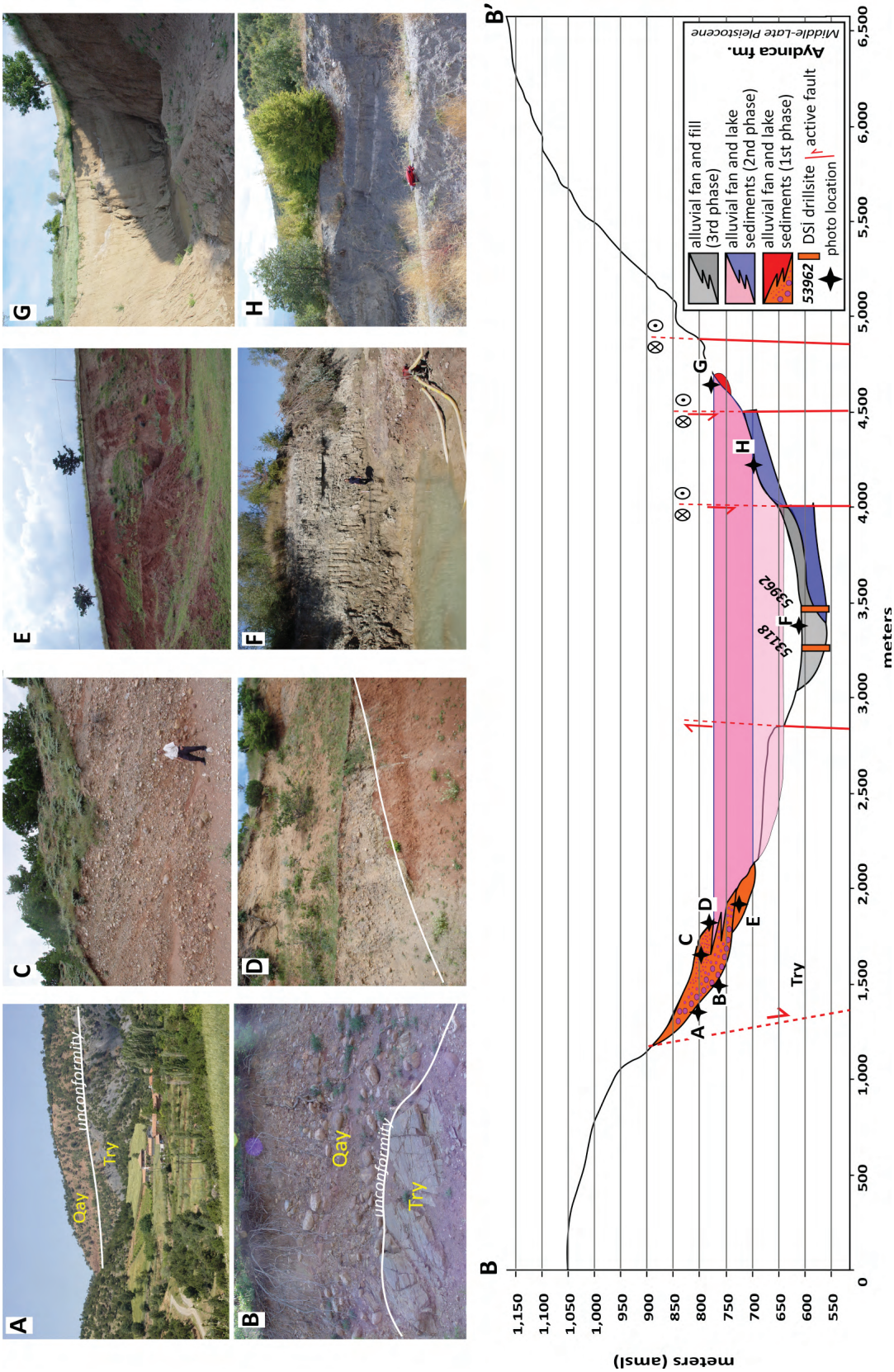

Figure 7. Simplified cross section (B–B' in Figure 6) showing the evolution steps of Aydınca Plain. The photographs correspond to the distributed lithofacies of the Aydınca formation (labelled A–H) located to the north and south of this fault-wedge basin, indicating different phases of sedimentation. The numbered orange bars indicate DSI (State Hydraulic Works) drilling sites from Karaalioğlu (1978). See text for details.

metamorphics, Try). The total measurable sedimentary thickness of the Aydınca formation, proposed to be ~350 metres, can be correlated with the subsidence in the Aydınca Plain. The amount of extension within the basin probably exceeds 2 km (Figure 7).

No age data have been obtained from the Aydınca formation as fine-grained sediments were washed away during erosional phases, making it impossible to find mammal fragments. Based on its stratigraphic position, we propose that the Aydınca formation started to accumulate synchronously with the initiation of the DF during the Mid–Late Pleistocene.

The southern drainage of the Aydınca Plain consists of linear and young rivers, but the steep topographic profiles of these rivers abruptly flatten as they approach the Deliçay River. The drainage network of the northern part is more mature and probably older than the initiation of the DF and the Aydınca Plain (Figure 6). There are neither morphological nor geological offset markers along the DF except for a 3.5±1 km offset of the Yeşilırmak River, measured by its cuts through gorges located south and north of the fault zone (Figure 6).

Geldingen Segment (GF)

The Geldingen Plain is a wide and complicated topographic flat (10 km in width and 20 km in length) at 420 m (amsl) average altitude, where 5 important headwaters (Yeşilırmak, Çekerek, Deliçay, Çorum and Efennik rivers) of the Yeşilırmak drainage system join to form the Yeşilırmak River. The active trace of the EzSF in the Geldingen Plain starts with a simple stepover of the DF in the east. This ~15-km-long E-trending single dextral fault strand (Geldingen Fault, GF) controls the formation of a narrow pull-apart basin (Geldingen Basin). South of the GF are also some NW-trending normal faults (Figure 8), which, together with the GF, control the actively subsiding part of the plain. The Neogene–Quaternary stratigraphy of the Geldingen Plain consists of three packages of sediments: (i) the Upper Miocene–Lower Pliocene Geldingen formation (Tg), (ii) the Upper Pleistocene river terraces (Qytr) and (iii) recent fluvial fill of the Geldingen pull-apart basin (Figures 8 & 10).

The Geldingen formation covers a wide area in the west of the basin and consists of fine- to coarse-grained clastics with imbricated pebbles, deposited in river channels and cross/parallel laminated coarse sand layers of longitudinal bar and banks. The major clast lithology is purple-coloured cherts, making the formation easily distinguishable from recent terrace deposits. *Nummulites* sp. fragments are also abundant in these fine-grained clastic rocks, indicating that the Lower–Middle Eocene neritic clastics and limestones of the Merzifon group (Keskin *et al.* 2008) were some of the primary clast sources. During the deposition of the Geldingen formation, visibly at least 250 metres thick, no clasts were derived from metamorphic rocks, especially blueschist facies rocks (Tüysüz 1996), exposed in the Karadağ uplift, where the Yeşilırmak formation (Try) is thrust over the Geldingen formation (Figure 9). Although it was impossible to construct primary relationships between different facies due to outcrop distribution and intense deformation, observed sedimentary features indicate that the Geldingen formation was deposited in a braided river environment. Discovery of an *Eomyidae keramidomys Carpathicus* rodent tooth (Schaub & Zapfe 1953) proves that the Geldingen formation is Upper Miocene–Lower Pliocene (MN13-14) in age.

The Geldingen formation was deformed twice. The first deformation phase controlled the deposition of the formation and was created by the E-trending, recently inactive Doğantepe-Figani branch of the Mecitözü Fault zone during the Early Miocene–Late Pliocene. The second phase, linked to the EzSF, caused post-depositional faulting and nearly vertical inclination of the formation close to the active faults. The original geometry of the formation also seems to be dissected by the active Geldingen pull-apart basin, which probably opened on the previous topographic flat filled by the Geldingen formation. Towards the western end of the plain, this deformation caused the development of the active Karadağ positive flower structure, bounded by active strands of the Mecitözü Fault in the north and by the Sungurlu Fault in the south (Figures 8 & 9). This also indicates a long (~3 Ma, Figure 6) non-depositional and erosional period in the central and western part of the EzSF (Figure 10).

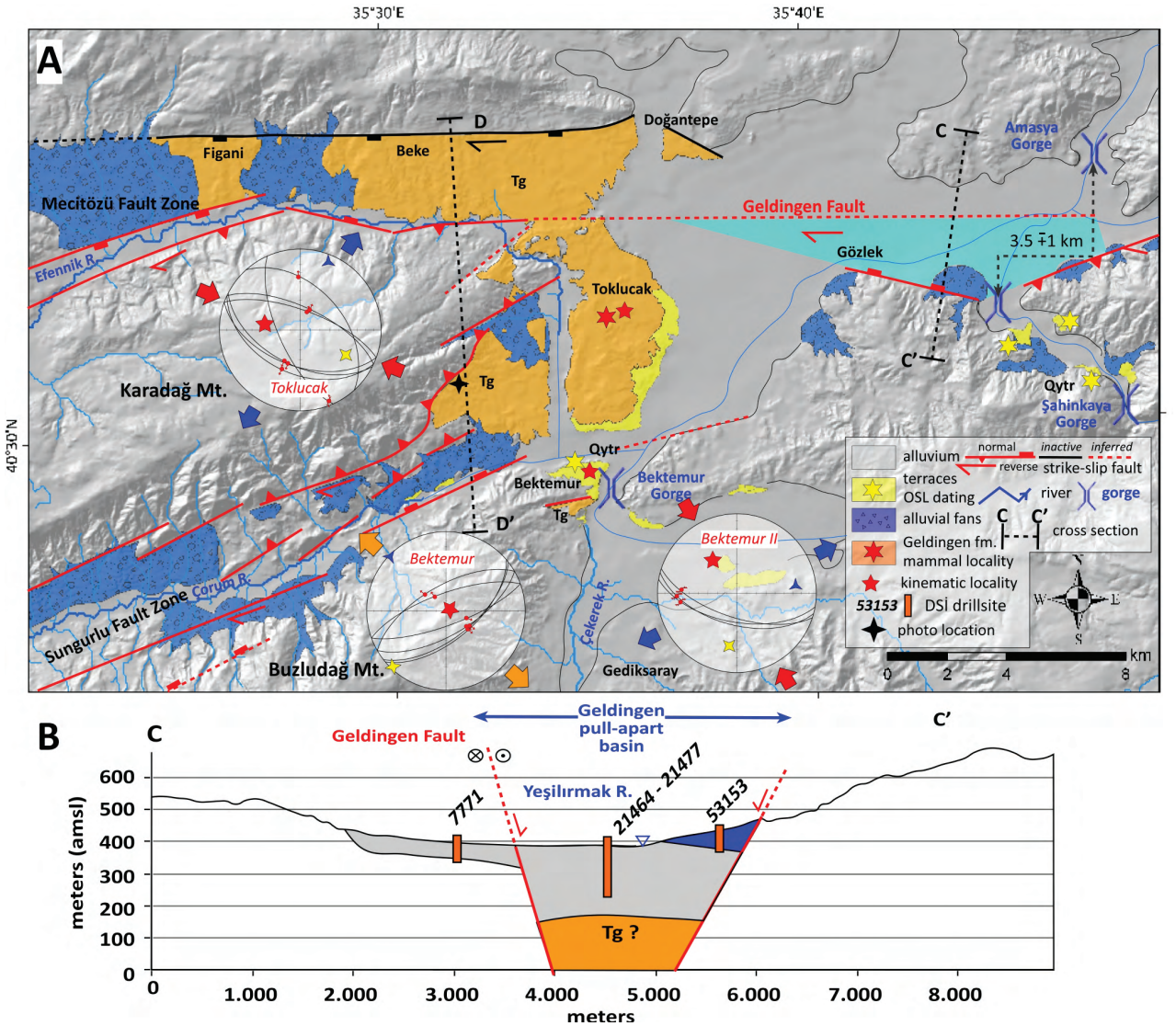

Figure 8. **(A)** Morphotectonic map along the Geldingen, Sungurlu and Mecitözü segments of the EzSFZ. Stereograms show the measured microfaults (Toklucak and Bektemur stations) and the results of the kinematic analysis. The Bektemur II data set is from Koçbulut (2003) and measured within the terrace sediments (Qytr). **(B)** Simplified geological interpretation of the cross section C–C'showing the pull-apart geometry of the Geldingen Basin. Numbered orange bars indicate DSI (State Hydraulic Works) drilling sites, from Karaalioğlu (1983).

The second sedimentary unit within the Geldingen Basin is the Upper Pleistocene terrace deposits formed along the gorges of the Yeşilırmak and the Çekerek rivers (Figure 8). These terraces are composed mainly of coarse bed-load gravels with sand lenses, resting unconformably on the Triassic basement in the east (Şahinkaya Gorge, Figure 8) and on the Geldingen formation in the west (Bektemur Gorge and Toklucak Village, Figure 8). OSL dates indicate that terrace formation in the west (Bektemur-Toklucak terraces) started at the beginning of the Late Glacial period (109.5±7.4 Ka, BKT03) and accumulated at least ~40 metres before 34.7±2.5 Ka ago (BKT01) (Kıyak & Erturaç 2008). The eastern terrace started to develop after an apparent delay (at around 47.0±2.2 Ka; AKS02), but then has a similar depositional history, which ended around 35.2±6.9 Ka ago (SHK01) (Kıyak & Erturaç 2008).

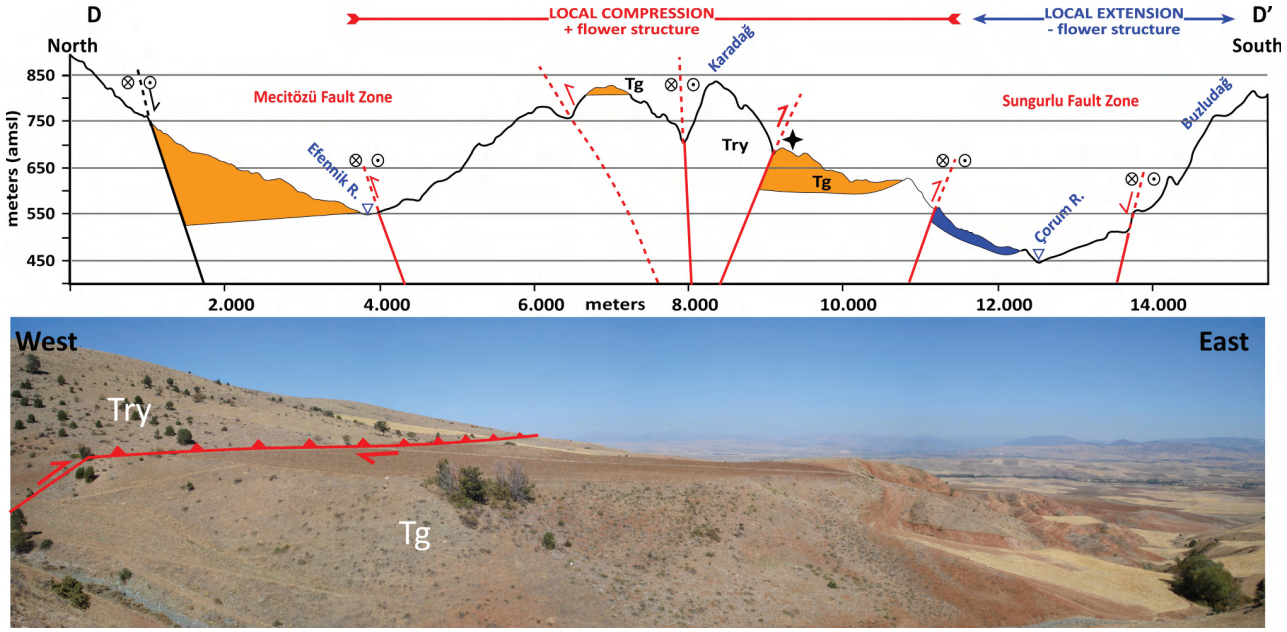

Figure 9. **(A)** Simplified cross section (D–D' in Figure-8) showing the effect of fault segmentation and geometry. The acute geometrical relationships between the GF, MF and SF created a positive flower structure (Karadağ Uplift) which was followed by a local extension (negative flower structure, Çorum River Valley) aligned in the same direction. **(B)** Panoramic photo looking NE where Triassic metamorphic rocks are thrust over Tg.

The sratigraphic base level of this terrace system is ~15–20 metres higher than the present floodplain, indicating a continuous base-level change due to rapid (2–4 mm/y) subsidence in the Geldingen pull-apart basin (Erturaç 2009). Post-depositional normal faults deform these terraces, as observed in sections near Bektemur Village (Figure 8), indicating post-35 Ka activity of the SF constrained by OSL dating (Kıyak & Erturaç 2008).

Sediment thickness and 3D geometry of the Geldingen Basin could not be ascertained in detail due to lack of borehole and geophysical data. Also, the few boreholes (IDs: 7771, 21467-21477, 53153; Karaalioğlu 1983) and seismic profiles (Akıncı *et al.* 1991) clustered around the Gözlek hot spring, close to the centre of the Geldingen Basin (Figure 8), show that the basin fill there is over 250 metres thick, but thins abruptly to the north of the recent plain. Based on this data and fault geometry along the basin border we can conclude that the Geldingen Basin formed as a pull-apart basin covering only a small part of the whole topographic plain (Figure 8).

The kinematics of the GF were determined by analyzing striated fault surfaces collected from outcrops of the Geldingen formation near Toklucak Village. The dataset consists of NNW-trending conjugate normal faults and NW-striking sinistral R' structures, which indicate that the GF formed in a dextral shear regime dominated by NNE–SSW-oriented extensional stress.

The GF ends north of the Toklucak Village, where it braches into two new fault segments: (i) E-trending Mecitözü Fault Zone (MFZ) and (ii) N65°E-trending Sungurlu Fault Zone (SFZ). In its NE part, the SFZ takes the form of parallel-trending and left-stepping active fault strands (Figure 8), which combine into a single strand towards the SW. The acute geometrical relationship between the GF and the SFZ forms a large restraining bend. This geometry obviously caused kinematic incompatibilities localized at the westernmost part of the Geldingen Plain, leading to the formation of distinctive morphotectonic features such as Karadağ Mountain and the Çorum River valley (Figure 8). Karadağ Mountain, bounded by the MFZ in the north and the SFZ in the south, formed as a positive flower structure under the control

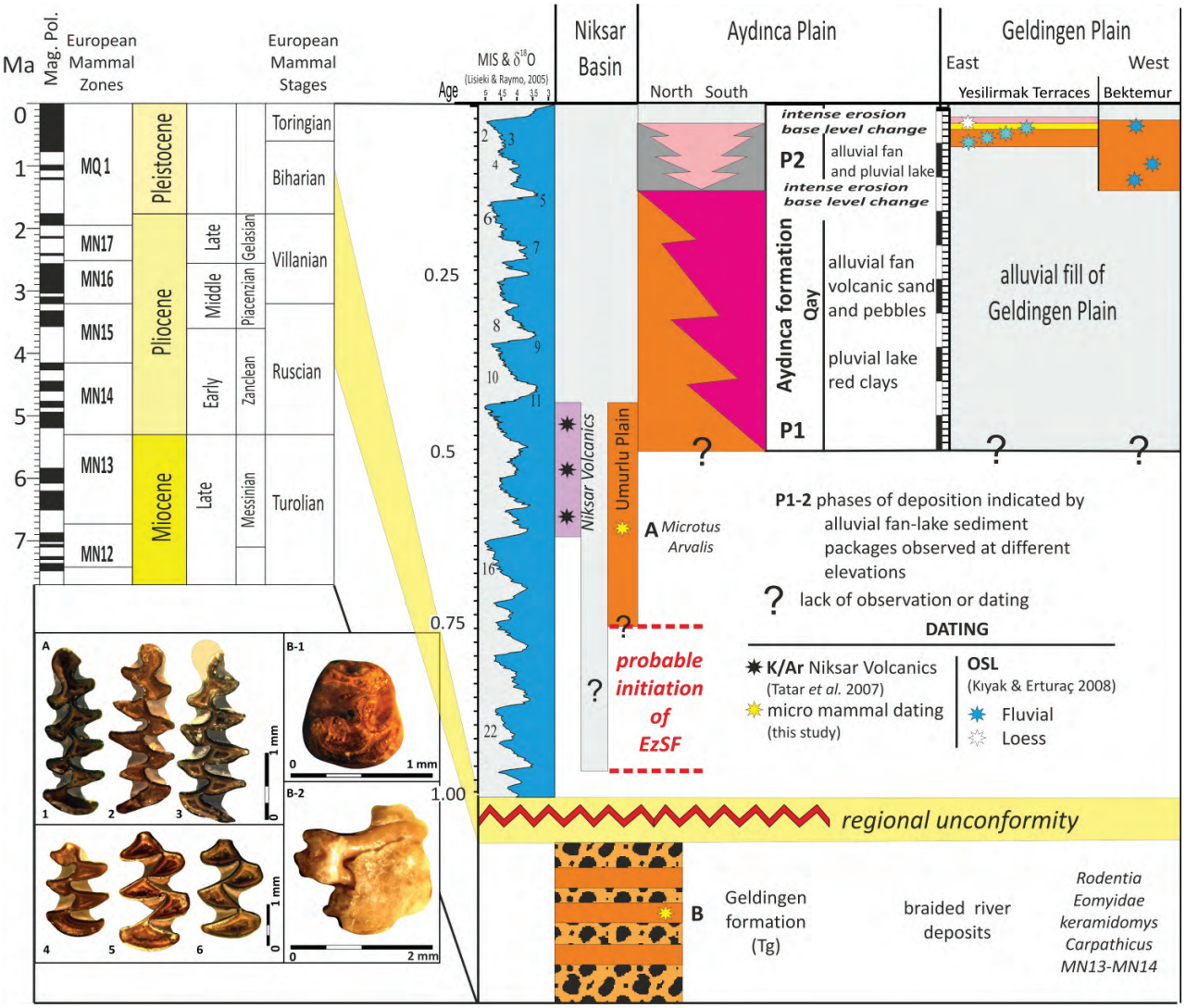

Figure 10. Generalized stratigraphic column of the Neogene–Quaternary stratigraphy of the study area (Amasya and partly Niksar Basins). Inset photographs **(A)** Occusal views of *Microtus* aff. *arvalis* (Pallas 1778) molars: M_1 (1-3), M_2 (4), M^1 (5), M^2 (6). **(A)** *Eomyidae Keramidomys carpathicus (*Schaub & Zapfe 1953) molar: occlusal view (1), lingual view (2). The end of the regional unconformity (~1 Ma) is proposed to be the initiation of the EzSF.

of NW–SE compression and strain partitioning between the MFZ and the SFZ. This structural anomaly is immediately balanced to the south, as the Çorum River valley forms a negative flower structure controlled by a local stress release with a NW–SE extension direction shown by kinematic analysis of the Bektemur fault dataset (Figures 8 & 11).

The SF is reported to be continuous southwestward to Kırıkkale Town (33.30°E, Şengör *et al.* 1985; Polat 1988; Şaroğlu *et al.* 1992). Here it displays a branched and anastomosing pattern rather than a narrow fault zone, especially beyond Sungurlu Town (34°E) (Seyitoğlu *et al.* 2009) where it has deformed Neogene deposits of the Çankırı Basin since the Late Miocene (Kaymakcı 2000). These data indicate that the system is older than the eastern parts of the EzSF, and also is a distributed deformation zone with very low seismic activity today.

Kinematics of the EzSF

To understand the properties and changes in the kinematics of the EzSF striated fault surfaces,

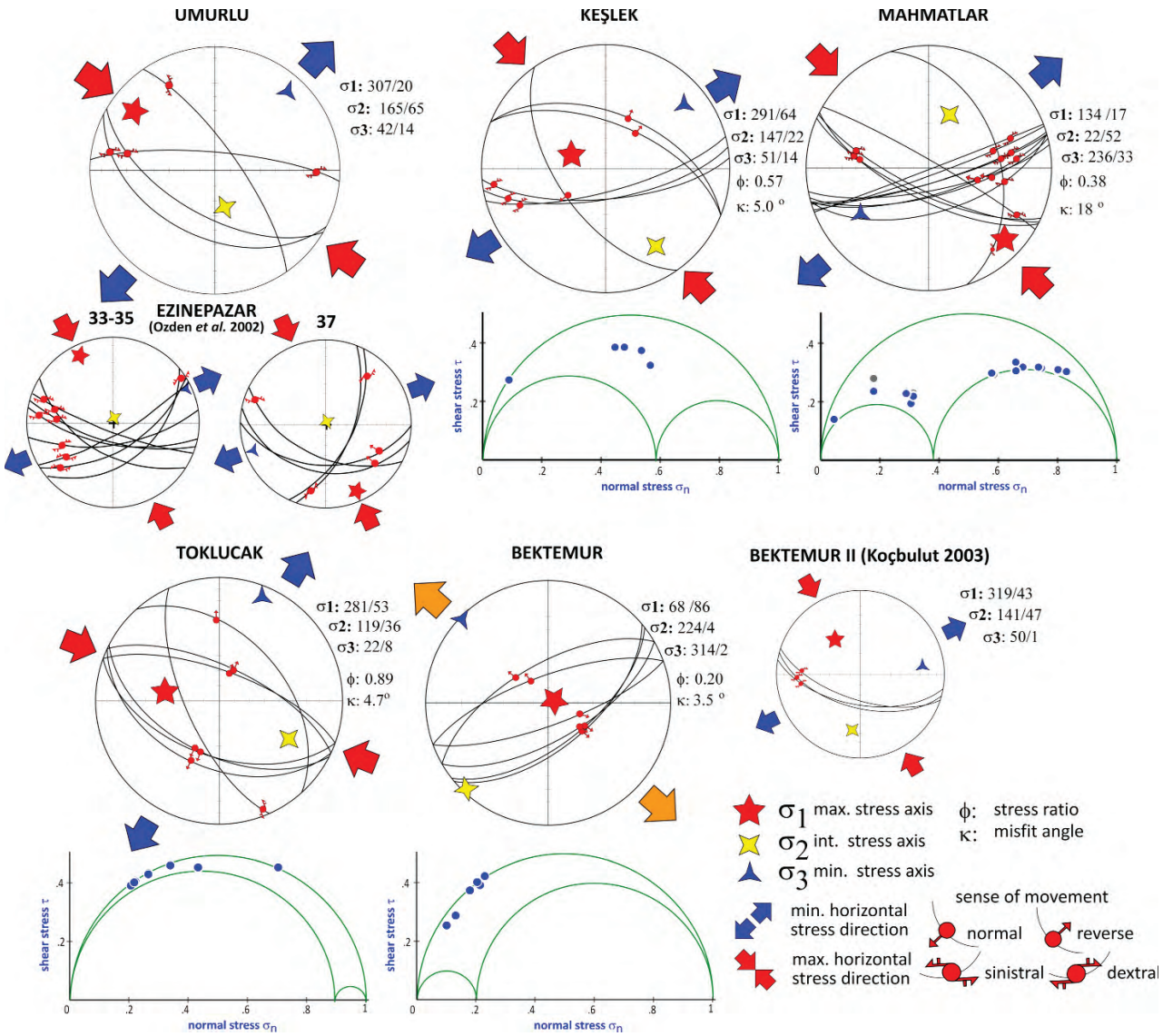

Figure 11. Derived principal stress directions and Mohr diagrams (inversion using minimized shear stress variation algorithm of Michael 1984) of microfault populations measured along the EzSF. The dextral fault set of the Bektemur II site is taken from Koçbulut (2003); see text for details.

deformed Neogene sediments only were measured and grouped according to their location and the relevant sedimentary unit. The faults observed within the palaeotectonic units were ignored to avoid mixing the different tectonic periods, as the EzSF is possibly a resurrected and/or replacement structure (see Şengör *et al.* 1985 for the terminology) of previous tectonic discontinuities. Locations and stereonet plots of these datasets along the EzSF are given in Figures 4, 6 and 8. The datasets, with enough (more than 6) measurements (Keşlek, Mahmatlar, Toklucak and Bektemur datasets) were analyzed by using the computational 'Minimized Shear Stress Variation' algorithm by Michael (1984) embedded in **MyFault© 1.03** (Pangea Scientific™) software, the others (Umurlu and Bektemur II datasets) were analyzed using the graphical 'Simple Shear Tensor Average' (also called P-T axis, Sunal & Tüysüz 2002) method of Turner (1953) using the **StereoNett© 2.46** software (Johannes 2000) with the methodology described in detail by Sunal & Tüysüz (2002). The results are presented in Figure 11 by means of principal stress

directions (σ_1= maximum, σ_2= intermediate and σ_3= minimum stress axes), stress ratios (Φ: $\sigma_2-\sigma_3/\sigma_1-\sigma_3$)), quality factors (mean slip misfit angle, κ) and Mohr diagrams.

Ezinepazar Segment

Due to limited Plio–Quaternary sedimentary exposures along the EzF, very few striated fault surfaces were measured in order to determine the actual stress tensor of this segment. The first dataset was measured from the NW end of the Umurlu Plain (also the mammal fossil locality) (Figure 4). It is composed of 4 striated faults measured in intensely sheared clastics including a conjugate set of 2 WNW-trending SW-dipping dextral faults with an W-trending north-dipping dextral fault (compatible with the southern border fault of the Umurlu Plain) and a NNW-trending NE-dipping sinistral fault (Figure 11A; Umurlu). All these faults have a slight normal component. The stress tensor is determined for this dataset using the P-T axis method (Turner 1953) and the results are σ_1= 307°/20°; σ_2= 165°/65°; σ_3= 42°/14°. We also used the available published kinematic datasets (sites 33–35 and 37 of Özden *et al.* 2002) to have a more constrained look (Figure 4). These datasets, which are measured in basement rocks, contain WNW- and WSW-directed, S- and SW-dipping dextral and NNE-trending sinistral faults (Figure 11B; sites 33-35 and 37), where some of these faults have a reverse component (Dataset 37). The calculated stress tensor of these datasets indicates a dextral shear zone with NNW-directed compressional and ENE-directed extensional horizontal stress directions. In this study, the master strand of the easternmost part of the EzF was determined to be a north-dipping dextral fault with reverse component, using its morphological signature. This interpretation regards the faults from Özden *et al.* (2002) as secondary structures (conjugates) to the master fault.

Deliçay Segment (DF)

Among many other unstriated faults observed in the sections along the DF, two datasets of striated fault surfaces could be analyzed. The first, the *Keşlek Dataset*, was collected from the sedimentary units deposited during the first phase of the Aydınca formation (Qay) and located north of the fault zone away from the active trace (Figure 6, Keşlek). The dataset consists of 6 measurements which can be grouped as NW-directed conjugate normal faults and nearly E-trending dextral faults allowing a very consistent (κ= 5.0°) computational stress analysis producing σ_1= 291°/64°, σ_2= 147°/22°, σ_3= 051°/14°. The horizontal stress directions and the stress ratio (Φ= 0.57) reveal an E–W-trending dextral transpressional stress regime (Figure 11C Keşlek). The *Mahmatlar Dataset* was collected from a section in intensely sheared clastic rocks of the Geldingen Formation (Tg), located on the active fault trace (Figure 6). The dataset consists of 8 ENE-trending and SW-dipping dextral faults with reverse component and a conjugate set of 4 NE-trending dextral faults with normal component which are very compatible with the saw tooth geometry of the DF (Figure 6). Also a NNW-trending E-dipping sinistral fault with reverse component was measured on a road cut, where basement rocks are thrust over the Tg, is included in the dataset. The computational analysis of this complicated dataset gives an eligible (κ= 18°) result with principal stress directions of σ_1= 134°/17°, σ_2= 022°/52°, σ_3= 236°/33°. The maximum and minimum stress directions are almost horizontal and the stress ratio (Φ= 0.38) indicates an E-trending transpressional dextral shear zone along the easternmost part of the DF (Figure 11D, Mahmatlar).

Geldingen-Sungurlu Segment

The sedimentary units along the western portion of the EzSFZ (Geldingen, Mecitözü and Sungurlu faults) do not give natural sections except in some aggregate quarries, where only few of them expose striated fault surfaces. The first, the *Toklucak Dataset,* was collected from a single section located east of Toklucak Village (also the mammal fossil locality) and to the S of the active trace of the GF (Figure 8). The dataset is composed of 5 ENE-trending conjugate normal faults and 2 NE-trending conjugate sinistral faults showing good consistency (κ= 4.7°) with each other. The kinematic analysis of this dataset gives σ_1= 281°/53°, σ_2= 119°/36°, σ_3= 022°/08° (Figure 11E, Toklucak). The directions of the principal stresses and the stress ratio (Φ= 0.89) together indicate a NNE-directed extension with a dextral component controlled by the GF. The faults forming the *Bektemur Dataset* were measured from the sections of an active

quarry, opened in Late Glacial terraces (Qtry) of the Çekerek River (Figure 8). Kinematic analysis of this homogenous and very consistent (κ= 3.5°) set of NE-trending conjugate normal faults produces σ_1= 068°/86°, σ_2: 224°/04°, σ_3= 314°/02° (Figure 11F, Bektemur). The directions of the principal stresses and the stress ratio (Φ= 0.20) together reveal a NW-directed extension with a slight sinistral component controlled by the Sungurlu Fault Zone (SFZ). This result indicates a clear extension direction reversal, incompatible with the proposed dextral nature of the SFZ (see detailed information and the literature list in previous sections). However, dextral faulting was also reported from the Bektemur location too (Figure 11G, Bektemur II; Koçbulut 2003). These observations, with three WNW-trending dextral faults, were not available to us in the field. As it was collected in an active quarry during the early 2000s, any visible trace has probably been erased since then. The stress directions, derived by geometrical analysis of these faults, have an orientation compatible with the proposed stress tensor controlling the SFZ (Figure 11F).

Discussion on the Results of the Kinematic Analysis

There is a good agreement between the kinematic datasets measured at the Umurlu, Keşlek, Mahmatlar and Toklucak stations indicating a pure E-trending dextral shear zone with a NE–SW extensional, and NW–SE compressional stress regime. Evidence for counterclockwise rotation in the stress tensor to the west is consistent with the trend of the fault zone tending to bend southwards. This was also reported from the western continuation of the ASZ, in the Çankırı Basin (Kaymakcı *et al.* 2003, deformation phase 3), where the total amount of rotation exceeds 45°. However, analysis of the Bektemur data, collected from the Late Glacial terraces deformed by the SFZ, shows clear NW–SE-oriented extension direction reversals with a vertical σ_1 direction. These reversals are probably caused by local stress release caused by geometric incompatibilities between the Sungurlu Fault and the current-day motion, as indicated by GPS vectors of the Central Anatolian Block (Figure 2). This phenomenon leads to a local compression at the eastern tip of the NE-directed SF master strand, which balances to the south with normal faulting parallel to the SF.

Historical and Instrumental Seismicity

Historical earthquake catalogues (Guidoboni *et al.* 1994; Ambraseys & Finkel 1995), report destructive earthquakes for the last two millennia, such as the AD 236, 1050, 1579, 1668 and 1794 events, within the extent of the ASZ. Limited damage information for these earthquakes is given for the major cities only, so it is not easy to distinguish the source fault. However, trenching studies (Yoshika *et al.* 2000; Hartleb *et al.* 2003, 2006) differentiated that the 236, 1050 and 1668 events ruptured the NAF, leaving at least two unlocated major earthquakes within the active faults of the ASZ. Also, Hartleb *et al.* (2006) attributed the 1579 event to movement on the EzF.

The instrumental seismicity catalogue of the study area (compiled using the ISC and KOERI Catalogues up to April, 2010) and the available focal mechanism solutions of the events (Tan *et al.* 2008; Çakır & Akoğlu 2008; Erturaç *et al.* 2009; Tan *et al.* 2010; INGV 2010) are presented in Figure 2. During the 20th Century, the northern boundary of the ASZ (NAF) completely ruptured with the 1942 (Mw= 7.1), 1943 (Mw= 7.2) and 1951 (M= 6.8) events. Although the eastern part of the fault zone shows a seismic quiescence; moderate-sized earthquakes (1966, Mb= 4.8 and 1977, Mb= 5.3) occurred on the NAF in the west between Tosya and Kurşunlu districts (Figure 2, Tan *et al.* 2008). The 2000 Orta Earthquake (Mw= 6.0) introduced a N-trending listric sinistral fault (Çakır & Akoğlu 2008) showing the complexity of the active deformation within the NASZ. Southwest of the ASZ, moderate-sized to large earthquakes occurred on WNW-trending dextral faults (Figure 2; 1938, Mw= 6.8; Tan *et al.* 2008 and 2005–2007, Ml= 5.6, Bala events; Tan *et al.* 2010). The seismicity within the ASZ is characterized by events up to M: 6.0, usually occurring in series of moderate-sized earthquakes on the active faults north of the EzSF (Figure 2), such as the 1942 Kızılırmak Valley (M= 5.6–6.0; Blumenthal *et al.* 1943; Eyidoğan *et al.* 1991), the successive 1996 Salhan (Mw= 5.7 and 5.6; HRV), 2005–2008 Çorum (M= 4.2–4.5; KOERI; Erturaç *et al.* 2009) and a very recent (02.04.2010; M= 4.5, INGV) earthquakes. The focal mechanism solutions of the recent events indicate NNE-directed sinistral faulting.

Apparent microseismic activity (events with magnitudes up to M= 4.0) occurs especially in the

eastern and central of parts of the EzSF (east of EzF and west of the DF, Figure 2). This pattern gradually scatters as the fault zone advances SW. The lack of focal mechanism solutions along the fault zone does not permit determination of the present-day stress tensor resolved on the EzSF.

Discussions and Conclusions

The EzSF is the first and longest dextral offshoot of the NAF west of the Karlıova triple junction and forms the southern boundary of an active wedge shaped deformation zone (ASZ). The morphology and geometry of this fault zone is not continuous; to the west its linear trend gradually becomes an en-échelon pattern, then branches into new faults.

The kinematics of these faults are determined by field observations, morphological signatures and also by using the analysis of microfault measurements which are accepted to obey the Coulomb-Mohr failure criterion and formed within the Riedel fracture geometry (Figure 3B, Tchalenko 1970; Dresen 1991). According to this statement, the E-, ENE- and WNW-oriented faults are dextral, whereas ENE-trending faults have reverse and WNW-trending faults have normal movement component. These faults correspond to the R, Y and P fractures forming the active trace of the EzSF. Sinistral faults, observed within the dextral shear zones of active faults (Mahmatlar and Toklucak Datasets) are oriented NNW. However, there is also distinctive left-lateral faulting, which are shown by the focal mechanisms of recent earthquakes located north of the EzSF (SaF in Figure 2). These N- and NNE-oriented faults correspond to the antithetic X shears, which are formed at an advanced stage in the continuous evolution of a shear zone (Dresen 1991).

The maximum morphological offset along the EzSF is measured at 6.5±0.5 km in the easternmost part of the Ezinepazar segment. Offset along the Deliçay and Geldingen segments is measured at 3.5±0.5 km by correlating the Yeşilırmak Gorge (Y-Y' in Figure 8). This trend of decreasing fault offsets is interpreted as showing slip on the EzSF terminating near Sungurlu Town, as supported by both GPS measurements (SNGR station from Yavaşoğlu *et al.* 2007) and offset markers on the Delice tributary of the Kızılırmak River (Şengör *et al.* 2005). This implies that the EzSF is a free tip ending fault system, such as the eastern Kunlun Fault (Kirby *et al.* 2007). The actual annual slip rate resolved on the fault shows a similar trend: ~7–10 mm/year for the easternmost part (morphological offset markers) and ~5 mm/year in the central part (Yavaşoğlu *et al.* 2011).

The geometrical changes along the course of the EzSF, led to the formation of various types of strike-slip basin. The stratigraphy of these basins implies two phases of fault-controlled sedimentation. The first phase controlled the Geldingen formation, dated as Late Miocene–Early Pliocene (MN 13-14, 6.5–4 Ma) with mammalian stratigraphy. The second phase started with the nucleation of the EzF around the Niksar Basin dated as Middle Pleistocene (~1–0.7 Ma) and migrated westward, forming the Aydınca and Geldingen basins (Figure 6).

Data presented in this paper show that the EzSF is a connection of a (i) replacement structure, EzF, which reactivated the older weak fault zones located within the Tokat Massif and a (ii) resurrected structure of an older intra-plate strike-slip system (the MF and the SF), which was active during the Miocene–Pliocene. This connection is established by the formation and westward migration of the EzF, which was probably initiated during the Middle Pleistocene and is still active today as a dextral fault zone forming part of a broad shear zone.

Acknowledgements

The authors are grateful to Şevket Şen (MNHN/Paris) for identifying the fossil fauna and Nafiye Güneç Kıyak (Işık Üniversity, Department of Physics) for dating the fluvial terraces. We wish to thank Robert Reilinger (MIT) for reviewing and correcting an early version of this manuscript. Comments from two anonymous referees clearly improved the ms. The Amasya Government is acknowledged for their invitation to study the geology of the area as a complement for Yeşilirmak River Basin Development Project (YHGP). This study is supported by İTÜ/BAP grant (No: 31982) and is part of the PhD Thesis by M. Korhan Erturaç (İTU/EIES).

References

Adiyaman, Ö., Chorowicz, J., Arnaud, N.O., Gündoğdu, M.N. & Gourgaud, A. 2001. Late Cenozoic tectonics and volcanism along the North Anatolian Fault: new structural and geochemical data. *Tectonophysics* **338**, 135–165.

Aktimur, T., Ateş, S., Yurdakul, E., Tekirli, E. & Kecer, M., 1992. Niksar-Erbaa ve Destek dolayının jeolojisi [Geology of Niksar-Erbaa and Destek regions]. *Mineral Research and Exploration Institute of Turkey (MTA) Bulletin* **114**, 25–37 [in Turkish].

Akinci, K, Karagöz, Ş., Gürer, A., Yenigün, H., Lezgi, A., Erzenoğlu, Z. & Yildirim, N. 1991. *Amasya-Gözlek Kaplıcası Sismik Etüd Raporu [Seismic Survey Report for Amasya-Gözlek Thermal Spring]*. Mineral Research and Exploration Institute of Turkey (MTA) Report no. **9200** [in Turkish, unpublished].

Akyüz, H.S., Hartleb, R., Barka, A.A., Altunel, E. & Sunal, G. 2002. Surface rupture and slip distribution of the 12 November 1999 Düzce earthquake (M 7.1), North Anatolian Fault, Bolu, Turkey. *Bulletin of Seismological Society of America* **92**, 61–66.

Allen, C.R. 1969. *Active Faulting in Northern Turkey*. Division Geological Sciences California Institute of Technolology, Contribution no. **1577**.

Alp, D. 1972. *The Geology of Amasya and Surroundings*. PhD Thesis, İstanbul University, Faculty of Science Monographs **22** [in Turkish].

Ambraseys, N.N. 1970. Some characteristic features of the North Anatolian Fault Zone. *Tectonophysics* **9**,143–65.

Ambraseys, N.N. & Finkel C.F. 1995. *The Seismicity of Turkey and Adjacent Areas—A Historical Review, 1500–1800*. Eren Yayıncılık, İstanbul.

Armijo, R., Meyer B., Hubert A. & Barka A.A. 1999. Westward propagation of the North Anatolian fault into the northern Aegean: timing and kinematics. *Geology* **27**, 267–270.

Barka, A.A. 1985. Geology and tectonic evolution of some Neogene-Quaternary basins in the North Anatolian Fault zone. *In: Ketin Symposium Book*. Publication of the Geological Society of Turkey, Ankara, 209–227 [in Turkish].

Barka, A.A. 1992. The North Anatolian Fault Zone. *Annales Tectonicae* **6**, 164–195.

Barka, A.A. 1996. Slip distribution along the North Anatolian Fault associated with large earthquakes of period 1939 to 1967. *Bulletin of the Seismological Society of America* **86**, 1238–1254.

Barka A.A. & Kadinsky-Cade, K. 1988. Strike-slip fault geometry in Turkey and its influence on earthquake activity. *Tectonics* **7**, 663–684.

Barka, A.A. & Gülen, L. 1989. Complex evolution of Erzincan Basin (eastern Turkey). *Journal of Structural Geology* **11**, 275–283.

Barka, A.A., Akyüz, S.H., Cohen, H.A. & Watchorn, F. 2000. Tectonic Evolution of the Niksar and Tasova-Erbaa pull-apart basins, North Anatolian Fault Zone: their significance for the motion of the Anatolian block. *Tectonophysics* **322**, 243–264.

Barka, A.A., Akyüz, H.S., Altunel, E., Sunal, G. & Çakir, Z. 2002. The surface rupture and slip distribution of the 17 August 1999 İzmit earthquake (M 7.4), North Anatolian Fault. *Bulletin of Seismological Society of America* **92**, 43–60.

Blumenthal, M.M. 1950. *Orta ve Aşağı Yeşilırmak Bölgelerinin (Tokat, Amasya, Havza, Erbaa, Niksar) Jeolojisi Hakkında [About the Geology of Central and Lower Yeşilırmak Regions (Tokat, Amasya, Havza, Erbaa, Niksar)]*. Mineral Research and Exploration Institute of Turkey (MTA) Geological Map Series **D/4**.

Blumenthal, M.M., Pamir, H.N. & Akyol, İ.H. 1943. Zur Geologie der Landstrecken der Erdbeben von ende 1942 in Nord-Anatolien und dortselbst ausgeführte makroseismische Beopachtungen [Şimal Anadolu zelzele sahasının jeolojisi ve 1942 yılı sonunda buralarda yapılan makro-sismik müşahedeleler]. *Mineral Research and Exploration Institute of Turkey (MTA) Bulletin* **29**, 33–58.

Bozkurt, E. 2001. Neotectonics of Turkey: a synthesis. *Geodinamica Acta* **14**, 3–30.

Bozkurt, E. & Koçyiğit, A. 1995. Almus Fault Zone: its age, total offset and relation to the North Anatolian Fault Zone. *Turkish Journal of Earth Sciences* **4**, 93–104.

Bozkurt, E. & Koçyiğit, A. 1996. The Kazova basin: an active negative flower structure on the Almus Fault Zone, a splay fault system of the North Anatolian Fault Zone, Turkey. *Tectonophysics* **265**, 239–254.

Christie-Blick, N. & Biddle, K. 1985. Deformation and basin formation along strike-slip faults. *In*: Christie-Blick, N. & Biddle, K. (eds), *Strike-slip Deformation, Basin Formation, and Sedimentation*. Society for Sedimentary Geology Special Publications. **37**, 1–35.

Çakir, Z. & Akoğlu, A.M. 2008. Synthetic aperture radar interferometry observations of the M= 6.0 Orta earthquake of 6 June 2000 (NW Turkey): reactivation of a listric fault. *Geochemistry Geophysics Geosystems* **9**, 2031.

Dhont, D., Chorowicz J., Yürür, T. & Köse, T. 1998. Polyphased block tectonics along the North Anatolian Fault in the Tosya basin area (Turkey). *Tectonophysics* **299**, 213–227.

Dresen, G. 1991. Stress distribution and the orientation of Riedel shears. *Tectonophysics* **188**, 239–247.

Erturaç, M.K. 2009. *Amasya ve Çevresinin Morfotektonik Evrimi [The Morphotectonic Evolution of Amasya and Sorroundings]*. PhD Thesis, İTÜ, Eurasia Institute of Earth Sciences, İstanbul [in Turkish with extended English summary].

Erturaç, M.K., Tüysüz, O., Özeren, S. & Çakir, Z. 2009. Kinematic evolution of the middle section of the convex Arc of the North Anatolian Fault: modelling a shear zone using GPS, INSAR and field data. *Geophysical Research Abstracts* **11**, EGU2009-8909-2.

Eyidoğan, H., Utku, Z., Güçlü, U. & Değirmenci, E. 1991. *Türkiye Büyük Depremleri Makro-Sismik Rehberi (1900–1988) [Macro-Siesmic Cataloque of Larger Earthquakes in Turkey (1900–1988)]*. İstanbul Technical University Publications, İstanbul [in Turkish with English abstract].

Flerit, F., Armijo, R., King, G.C.P., Meyer, B. & Barka, A.A. 2003. Slip partitioning in the Sea of Marmara pull-apart determined from GPS velocity vectors. *Geophysical Journal International* **154**, 1–7.

Hartleb, R.D., Dolan, J.F., Akyüz, H.S. & Yerli, B. 2003. A 2,000 year-long paleoseismologic record of earthquakes along the central North Anatolian fault, from trenches at Alayurt, Turkey. *Bulletin of the Seismological Society of America* **93**, 1935–1954.

Hartleb, R.D., Dolan, J.F., Kozaci, Ö., Akyüz, H.S. & Seitz, G.G. 2006, A 2500-yr-long paleoseismologic record of large, infrequent earthquakes on the North Anatolian fault at Çukurçimen, Turkey. *Geological Society of America Bulletin* **118**, 823–840.

Hempton, M.R. & Dunne, L.A. 1984. Sedimentation in pull-apart basins: active examples in Eastern Turkey. *Journal of Geology* **92**, 513–30.

Herece, E. & Akay, E. 2003. *Atlas of North Anatolian Fault (NAF), 1:100000 Scale*. Mineral Research and Exploration (MTA) Special Publication, Ankara, Turkey.

Hrv 2010. *Harvard University, Global Centroid Moment Tensor Catalogue*. http://www.globalcmt.org/CMTsearch.html.

Huang, W. 1993. Morphological patterns of stream channels on the active Yishi Fault, southern Shandong Preovince, Eastern China: implications for repeated great earthquakes in the Holocene. *Tectonophysics* **213**, 283–304.

Guidoboni, E., Comastri, A. & Triana A.G. 1994. *Catalogue of Ancient Earthquakes in the Mediterranean Area up to the 10th century*. Instituto Nazionale di Geofisica, Rome, ISBN 88-85213-06-5.

Gürer, Ö.F., Sanğu, E. & Özburan, M. 2006. Neotectonics of the SW Marmara region, NW Anatolia, Turkey. *Geological Magazine* **143**, 229–241.

Isc 1999. *International Seismological Centre: On-line Bulletin*. http://www. isc.ac.uk/Bull, International Seismological Centre, Thatcham, United Kingdom.

Ingv 2010. *Istituto Nazionale di Geofisica e Vulcanologia*. http://earthquake.rm.ingv.it /data_id/2211706441/qrcmt.fin.

İşseven, T. & Tüysüz, O. 2006. Palaeomagnetically defined rotations of fault-bounded continental blocks in the North Anatolian Shear Zone, North Central Anatolia. *Journal of Asian Earth Sciences* **28**, 469–479.

Johannes, D. 2000. *StereoNett Version 2.46*. Shareware Copyrighted Software.

Karaalioğlu, B. 1978. *Hydrogeological Investigation Report of Aydınca Ezinepazar Plain*. General Directorate of State Hydraulic Works (DSİ) Report, Ankara [in Turkish].

Karaalioğlu, B. 1983. *Hydrogeological Investigation Report of Geldingen Plain*. General Directorate of State Hydraulic Works (DSİ) Report, Ankara [in Turkish].

Kaymakci, N. 2000. *Tectono-stratigraphical Evolution of the Çankırı Basin (Central Anatolia, Turkey)*. PhD. Thesis, Utrecht University, The Netherlands. Geologica Ultraiectina.

Kaymakci, N., White, S.H. & van Dijk P.M. 2003. Kinematic and structural development of the Çankırı Basin (Central Anatolia, Turkey): a paleostress inversion study. *Tectonophysics* **364**, 85–113.

Kaymakci, N., Özmutlu, Ş., Van Dijk P.M. & Özçelik, Y. 2010. Surface and subsurface characteristics of the Çankırı Basin (Central Anatolia, Turkey): integration of Remote Sensing, seismic interpretation and gravity. *Turkish Journal of Earth Sciences* **19**, 79–100.

Keskin, M., Genç, S.C. & Tüysüz, O. 2008. Petrology and geochemistry of post-collisional Middle Eocene volcanic units in North-Central Turkey: evidence for magma generation by slab breakoff following the closure of the Northern Neotethys Ocean. *Lithos* **104**, 267–305.

Ketin, İ. 1957. Kuzey Anadolu deprem fayı [North Anatolian earthquake fault]. *Bulletin of İstanbul Technical University* **15**, 49–52 [in Turkish].

Ketin, İ. 1969. Über die nordanatolische Horizontalverschiebung. *Mineral Research and Exploration Institute of Turkey (MTA) Bulletin* **72**, 1–28.

Kim, Y.S. & Sanderson, D.J. 2006. Structural similiarity and variety at the tips in a wide range of strike-slip faults: a review. *Terra Nova* **18**, 330–344.

Kiratzi, A.A. 2002. Stress tensor inversions along the westernmost North Anatolian Fault Zone and its continuation into the Aegean Sea. *Geophysical Journal International* **151**, 360–376.

Kirby, E., Harkins, N., Wang, E., Shi, X., Fan, C. & Burbank, D. 2007. Slip rate gradients along the eastern Kunlun fault. *Tectonics* **26**, 2010–2026.

Kiyak, N.G. & Erturaç, M.K. 2008. Luminescence ages of feldspar contaminated quartz from fluival terrace sediments. *Geochronometria* **30**, 55–60.

Koeri 2010. *Bogazici University, Kandilli Observatory and Earthquake Research Institute, On-line Bulletin*. http://www.koeri.boun.edu.tr/sismo/Mudim /katalog.asp, İstanbul, Türkiye.

Koçbulut, F. 2003. *Göynücek-Gediksaray Kuzeyinde (GB Amasya) Ezinepazar-Sungurlu Fayı'nın Neotektonik Özellikleri [Neotectonic Characteristics of the Ezinepazar-Sungurlu Fault in the Northern Part of Göynücek-Gediksaray Region (SW Amasya)]*. PhD Thesis, Sivas Cumhuriyet University, Institute of Natural Sciences [in Turkish with English abstract].

Koçyiğit, A. 1989. Suşehri basin: an active fault wedge basin on the North Anatolian Fault Zone, Turkey. *Tectonophysics* **167**, 13–29.

Koçyiğit, A. 1990. Tectonic setting of the Gölova Basin: total offset of the North Anatolian Fault Zone, E Pontide, Turkey. *Annales Tectonicae* **4**, 155–170.

Koçyiğit A. 1996. Superimposed basins and their relations to the recent strike-slip fault zone: a case study of the Refahiye superimposed basin adjacent to the North Anatolian Transform Fault, northeastern Turkey. *International Geology Review* **38**, 701–713.

Koçyiğit, A. 2003. Orta Anadolu'nun genel tektonik özellikleri ve depremseliği [General tectonic characteristics and seismicity of Ankara region]. *Turkish Association of Petroleum Geologists Bulletin*, *Special Publication* **5**, 1–26 [in Turkish with English abstract].

Koçyiğit, A. & Beyhan A. 1998. A new intracontinental transcurrent structure: the Central Anatolian Fault Zone, Turkey. *Tectonophysics* **284**, 317–36.

Koçyiğit, A., Rojay, B., Cihan, M. & Özacar, A. 2001. The June 6, 2000 Orta (Çankırı, Turkey) earthquake: sourced from a new antithetic sinistral strike-slip structure of the North Anatolian Fault system, the Dodurga Fault Zone. *Turkish Journal of Earth Sciences* **10**, 69–82.

Kozaci, Ö., Dolan, J., Finkel, R. & Hartleb, R. 2007. Late Holocene slip rate for the North Anatolian fault, Turkey, from cosmogenic ^{36}Cl geochronology: implications for the constancy of fault loading and strain release rates. *Geology* **35**, 867–870.

Mann, P., Hempton, M.R., Bradley, D.C. & Burke, K. 1983. Development of pull-apart basins. *Journal of Geology* **91**, 529–554.

McClay, K. & Bonora, M. 2001. Analog models of restreaning stepovers in strike-slip fault systems. *American Association of Petroleum Geologists Bulletin* **85**, 233–260.

McClusky, S.C., Balassanian, S., Barka, A.A., Ergintav, S., Georgiev, I., Gürkan, O., Hamburger, M., Hurst, K., Kahle, H., Kastens, K., Kekelidse, G., King, R., Kotzev, V., Lenk, O., Mahmoud, S., Mishin, A., Nadaria, M., Ouzounis, A., Paradisissis, D., Peter, Y., Prilepin, M., Reilinger, R.E., Şanli, I., Seeger, H., Teableb, A., Toksöz, N. & Vei, G. 2000. Global Positioning System constraints on plate kinematics and dynamics in the eastern Mediterranean and Caucasus. *Journal of Geophysical Research* **105**, 5695–5719.

McKenzie, D.P. 1972. Active tectonics of the Mediterranean region. *Geophysical Journal of Royal Astronomical Society* **30**, 109–185.

McKenzie, D.P. & Jackson, J.A. 1986. A block model of distributed deformation by faulting. *Journal of the Geological Society, London,* **143**, 349–353.

Meade, B.J., Hager, B.H., McClusky, S.C., Reilinger, R.E. & Ergintav, S. 2002. Estimates of seismic potential in the Marmara Sea region from block models of secular deformation constrained by Global Positioning System measurements. *Bulletin of Seismological Society of America* **92**, 208–215.

Michael, A.J. 1984. Determination of stress from slip data: faults and folds. *Journal of Geophysical Research* **89**, 11517–11526.

Naylor, M.A., Mandl, G. & Sijpesteijn, C.H.K. 1986. Fault geometries in basement-induced wrench faulting under different initial stress states. *Journal of Structural Geology* **8**, 737–752.

Okay, A.I., Zattin, M. & Cavazza, W. 2010. Apatite fission-track data for Miocene Arabia-Eurasia collision. *Geology* **38**, 35–38.

Özden, S., Över, S., & Ünlügenç, U.C. 2002. Quaternary stress regime change along the eastern North Anatolian Fault Zone, Turkey. *International Geology Review* **44**, 1037–1052.

Parejas, E., Akyol, İ.H. & Altinli, E. 1941. Le tremblement de terre d'Erzincan du 27 décembre 1939 (Secteur occidental). *İstanbul Üniversitesi Jeoloji Entitüsü Dergisi* **10**, 187–222.

Pinar, A., Kalafat, D. & Üçer, S.B. 1998. Rayleigh yüzey dalga spekturumu, cisim dalgaları ve ilk hareket yönlerinden 1992–1997 yıllarında oluşan depremlerin (Ms= 5.5–6.8) analizi [Analysis of 1992–1997 earthquakes (Ms= 5.5–6.8) based on Rayleigh surface wave spectrum, body waves and aspects of the first movement]. *Deprem Araştırma Bülteni* **76**, 88–122 [in Turkish with English abstract].

Polat, A. 1988. Büyük Polat-Yarımsöğüt (Sungurlu-Çorum) yöresinde paleotektonik ve neotektonik geçiş döneminin izleri ve Kırıkkale-Erbaa fay zonunun oluşumu [Evidence for palaeo- to neo-tectonic transition period in the Büyük Polat-Yarımsöğüt (Sungurlu-Çorum) region and the origin of the Kırıkkale-Erbaa fault zone]. *Turkish Association of Petroleum Geologists Bulletin* **1**, 127–140 [in Turkish with English abstract].

Pucci, S., Palyvos, N., Zabci, C., Pantosti, D. & Barchi, M. 2006. Coseismic ruptures and tectonic landforms along the Düzce segment of the North Anatolian Fault Zone (Ms 7.1, Nov. 1999). *Journal of Geophysical Research* **111**, B06312.

Pucci, S., De Martini, P.M. & Pantosti, D. 2008. Preliminary slip rate estimates for the Düzce segment of the North Anatolian Fault Zone from offset geomorphic markers. *Geomorphology* **97**, 538–554.

Ramsey, J.G. & Lisle, R.J. 2000. *The Techniques of Modern Structural Geology, Volume 3: Application of Continuum Mechanics in Structural Geology*. Academic Press Limited, London.

Reilinger, R., McClusky, S., Vernant, P., Lawrence, S., Ergintav, S., Çakmak, R., Özener, H., Kadirov, F., Guliev, I., Stepanyan, R., Nadariya, M., Hahubia, G., Mahmoud, S., Sakr, K., ArRajehi, A., Paradissis, D., Al-Aydrus, A., Prilepin, M., Guseva, T., Evren, E., Dmitrotsa, A., Filikov,S.V., Gomez, F., Al-Ghazzi, R. & Karam, G. 2006. GPS constraints on continental deformation in the Africa-Arabia-Eurasia continental collision zone and implications for the dynamics of plate interactions. *Journal of Geophysical Research* **111**, B05411.

Rojay, B. 1993. *Tectonostratigraphy and Neotectonic Characteristics of the Southern Margin of Merzifon-Suluova Basin (Central Pontides, Amasya)*. PhD Thesis, Middle East Technical University, Ankara [unpublished].

Rojay, B. 1995. Post-Triassic evolution of Central Pontides: evidence from Amasya region, Northern Anatolia. *Geologica Romana* **31**, 329–350.

Rotstein, Y. 1984. Counterclockwise rotation of the Anatolian Block. *Tectonophysics* **108**, 71–91.

Sala, B. & Masini, F. 2007. Late Pliocene and Pleistocene small mammal chronology in the Italian peninsula. *Quaternary International* **160**, 4–16.

Suzanne, P. & Lyberis, N. 1992. Mechanisme de deformation le long de la partie orientale de la Faille Nord Anatolienne. *Annales Tectonicae* **6**, 26–41.

Şaroğlu, F., Emre, Ö. & Kuşçu, İ. 1992. *Active Fault Map of Turkey at 1:2,000,000 Scale*. Mineral Research and Exploration Institute of Turkey (MTA) Publications, Ankara.

Schaub, S. & Zapfe. H. 1953. Die Fauna der Miozanen Spaltenfullung von Neudorf an der March, Simplicidentata. *Sitzungsberichte der Österreichische Akademie der Wissenschaften, Mathematisch Naturwissenschaftliche Klasse Abteilung* **162**, 181–215.

Şenel, M. 2002. *Geological Map of Turkey, Samsun Sheet at 1:500.000 Scale*. Mineral Research and Exploration Institute of Turkey (MTA) Publications, Ankara.

Şengör, A.M.C. 1979. The North Anatolian Transform Fault: its age, offset and tectonic significance. *Journal of the Geological Society, London* **139**, 269–282.

Şengör, A.M.C. & Barka, A.A. 1992. Evolution of escape related strike slip systems: implications for disruption of collusional orogens. *29th International Geological Congress, 21 August-3 September, 1992, Kyoto Japan, Abstracts* **1**, I-2-56, O-1, 1721.

Şengör, A.M.C, Görür, N. & Şaroğlu, F. 1985. Strike slip faulting and related basin formation in zones of tectonic escape: Turkey as a case study. *In*: Christie-Blick, N. & Biddle, K. (eds), *Strike-slip Deformation, Basin Formation, and Sedimentation*. Society of Economic Paleontologists and Mineralogists, Special Publications **37**, 227–64.

Şengör, A.M.C., Tüysüz, O., İmren, C., Sakınç, M., Eyidoğan, H., Görür, N., Le Pichon X. & Rangin, C. 2005. The North Anatolian Fault: a new look. *Annual Review Earth Planetary Sciences* **33**, 1–75.

Şengör, A.M.C. & Yilmaz Y. 1981. Tethyan evolution of Turkey: A plate tectonic approach. *Tectonophysics* **75**, 181–243.

Seyitoğlu, G., Kazanci, N., Karadenizli, L., Şen, Ş., Varol, B. & Karabiyikoğlu, T. 2000. Rockfall avalanche deposits associated with normal faulting in the NW of Çankırı basin: implication for the post-collisional tectonic evolution of the Neo-Tethyan suture zone. *Terra Nova* **12**, 245–251.

Seyitoğlu, G., Aktuğ, B., Karadenizli, L., Kaypak, B., Şen, Ş., Kazanci, N., Işik, V., Esat, K., Parlak, O., Varol, B., Saraç, G. & İleri, İ. 2009. A Late Pliocene–Quaternary pinched crustal wedge in NW Central Anatolia, Turkey: a neotectonic structure accommodating the internal deformation of the Anatolian Plate. *Geological Bulletin of Turkey* **52**, 121–154.

Sunal, G. & Tüysüz, O. 2002. Paleo-stress analyses of Tertiary post-collisional structures in the Western Pontides: northern Turkey. *Geological Magazine* **139**, 343–359.

Tan, O., Tapirdamaz, C. & Yörük, A. 2008. The Earthquake Catalogues for Turkey. *Turkish Journal of Earth Sciences* **17**, 405–418.

Tan, O., Tapirdamaz, M.C., Ergintav, S., İnan, S., İravul, Y., Saatçilar, R., Tüzel, B., Tarancioğlu, A., Karakisa, S., Kartal, R.F., Zünbül, S., Yanik, K., Kaplan, M., Şaroğlu, F., Koçyiğit, A., Altunel, E. & Özel, N.M. 2010. Bala (Ankara) earthquakes: implications for shallow crustal deformation in Central Anatolian section of the Anatolian platelet (Turkey). *Turkish Journal of Earth Sciences* **19**, 449–471.

Tatar, O. 1996. Neotectonic structures indicating extensional and contractional strain within Pliocene deposits near the NW margin of the Niksar pull-apart basin, Turkey. *Turkish Journal of Earth Sciences* **5**, 81–90.

Tatar, O., Piper, J.D.A., Graham, P.R. & Gürsoy, H. 1995. Palaeomagnetic study of block rotations in the Niksar overlap region of the North Anatolian Fault Zone, central Turkey. *Tectonophysics* **244**, 251–66.

Tatar, O., Yurtmen, S, Temiz, H., Koçbulut, F., Mesci, L. & Guezou J.C. 2007. Intracontinental Quaternary volcanism in the Niksar pull-apart basin, North Anatolian Fault Zone, Turkey. *Turkish Journal of Earth Sciences* **16**, 417–440.

Tchalenko J.S. 1970. Similarities between shear zones of different magnitudes. *Geological Society of America Bulletin* **81**, 1625–1640.

Turner, F.J. 1953. Nature and dynamic interpretation of deformation lamellae in calcite of three marbles. *American Journal of Science* **251**, 276–98.

Tüysüz, O. 1992. *The Geological Maps of Çorum G-35-c and G-35-d Quadrangles at 1/50.000 Scale*. Turkish Petroleum Corporation (TPAO) map [unpublished].

Tüysüz, O. 1996. Amasya ve çevresinin jeolojisi [Geology of Amasya and its surroundings]. *Türkiye 11. Petrol Kongresi. Proceedings*, Ankara, 32–48 [in Turkish with English abstract].

Tüysüz, O., Yiğitbaş, E., Genç, T. & Tari, U. 1998. *Batı Karadeniz Bölgesinin Tektonik Birliklerinin Ayırdı ve 1: 500.000 Ölçekli Jeoloji Haritasının Hazırlanması [Tectonic Units of Western Black Sea Region and Their Geological Mapping at 1: 500.000 Scale]*. TÜBİTAK Project Report **YDABÇAG-17** [in Turkish with English abstract, unpublished].

Westaway, R. & Arger, J. 2001. Kinematics of the Malatya-Ovacık fault zone. *Geodinamica Acta* **14**, 103–31.

Yavaşoğlu, H., Tari, E., Karaman, H., Şahin, M., Baykal, O., Erden, S., Bilgi, S., Rüzgar, G., İnce, C.D., Ergintav, S., Çakmak, R., Tari, U. & Tüysüz, O. 2007. GPS Measurements along the North Anatolian Fault on the Mid-Anatolia segment. *In Geodetic Deformation Monitoring: From Geophysical to Engineering Roles,* 166–171. Springer Berlin Heidelberg.

Yavaşoğlu, H., Tari, E., Tüysüz, O., Çakir, Z. & Ergintav, S. 2011. Determining and modeling tectonic movements along the central part of the North Anatolian Fault (Turkey) using Geodetic Measurements. *Journal of Geodynamics* **51**, 339–343.

Yilmaz, Y., Serdar, H.S., Genç, C. Ş., Yiğitbaş, E., Gürer, Ö.F., Elmas, A., Yildirim, M., Bozcu, M. & Gürpinar, O. 1997. The geology and evolution of the Tokat Massif, south-Central Pontides, Turkey. *International Geology Review* **39**, 365–382.

Yilmaz, A. & Yilmaz, H. 2004. Geology and structural evolution of the Tokat Massif (Eastern Pontides, Turkey). *Turkish Journal of Earth Sciences* **13**, 231–246.

Yoshika, T., Okumura, K, Kuşçu, İ. & Emre, Ö. 2000. Recent surface faulting of the North Anatolian Fault along the 1943 Ladik earthquake ruptures. *Bulletin of the Geological Survey of Japan* **51**, 29–35.